



Original article

27-Hydroxycholesterol/liver X receptor/apolipoprotein E mediates zearalenone-induced intestinal immunosuppression: A key target potentially linking zearalenone and cancer

Haonan Ruan, Jing Zhang, Yunyun Wang, Ying Huang, Jiashuo Wu, Chunjiao He, Tongwei Ke, Jiaoyang Luo^{**}, Meihua Yang^{*}

Key Laboratory of Bioactive Substances and Resources Utilization of Chinese Herbal Medicine, Ministry of Education, Institute of Medicinal Plant Development, Chinese Academy of Medical Sciences & Peking Union Medical College, Beijing, 100193, China



ARTICLE INFO

Article history:

Received 10 March 2023

Received in revised form

7 July 2023

Accepted 7 August 2023

Available online 9 August 2023

Keywords:

Zearalenone

Intestinal immunosuppression

Apolipoprotein E

Bioinformatics analysis

Cancer

ABSTRACT

Zearalenone (ZEN) is a mycotoxin that extensively contaminates food and feed, posing a significant threat to public health. However, the mechanisms behind ZEN-induced intestinal immunotoxicity remain unclear. In this study, Sprague-Dawley (SD) rats were exposed to ZEN at a dosage of 5 mg/kg/day b.w. for a duration of 14 days. The results demonstrated that ZEN exposure led to notable pathological alterations and immunosuppression within the intestine. Furthermore, ZEN exposure caused a significant reduction in the levels of apolipoprotein E (ApoE) and liver X receptor (LXR) ($P < 0.05$). Conversely, it upregulated the levels of myeloid-derived suppressor cells (MDSCs) markers ($P < 0.05$) and decreased the presence of 27-hydroxycholesterol (27-HC) in the intestine ($P < 0.05$). It was observed that ApoE or LXR agonists were able to mitigate the immunosuppressive effects induced by ZEN. Additionally, a bioinformatics analysis highlighted that the downregulation of ApoE might elevate the susceptibility to colorectal, breast, and lung cancers. These findings underscore the crucial role of the 27-HC/LXR/ApoE axis disruption in ZEN-induced MDSCs proliferation and subsequent inhibition of T lymphocyte activation within the rat intestine. Notably, ApoE may emerge as a pivotal target linking ZEN exposure to cancer development.

© 2023 The Authors. Published by Elsevier B.V. on behalf of Xi'an Jiaotong University. This is an open access article under the CC BY-NC-ND license (<http://creativecommons.org/licenses/by-nc-nd/4.0/>).

1. Introduction

Zearalenone (ZEN) is a mycotoxin produced by fungi of the *Fusarium* genus [1] and is commonly present in crops such as wheat, soybeans, and corn [2]. It is frequently detected as a contaminant in maize, legumes, and feed mixes, with contamination rates exceeding 75% and a maximum concentration of 1,560 µg/kg [3]. ZEN exhibits estrogenic effects and is known to cause reproductive toxicity [4] and hepato-renal toxicity [5] in humans. To regulate its presence, most countries and organizations have established maximum residue limits for ZEN in food and feed [6]. Human exposure is typically close to the provisional maximum tolerable daily intake of 0.5 µg/kg/day b.w. for the total intake of ZEN and its metabolites, as indicated by numerous studies [7,8]. The

International Agency for Research on Cancer has classified ZEN as Group 3, meaning it is not classifiable regarding its carcinogenicity to humans [9].

In addition to its impact on estrogenic compounds in the human body, ZEN can disrupt other endocrine metabolites and cause toxicity by affecting their corresponding nuclear receptors and downstream targets [10]. Metabolomic data from *in vitro* culture models of porcine follicles exposed to ZEN (0, 3, 10, and 30 µM, 12 days) revealed a depletion of lysophosphatidylcholine accumulation during follicle growth [11]. Furthermore, hepatic lipidomics and serum metabolomics conducted after ZEN exposure in mice (2 mg/kg/day b.w., i.g., 63 days) demonstrated disturbances in hepatic lipid metabolism [12]. Additionally, metabolomic and transcriptomic analyses on porcine intestinal epithelial cells exposed to ZEN (10 µg/mL, 24 h) revealed significant effects on lipid metabolism [13].

ZEN has also been shown to exhibit immunotoxicity [14] and intestinal toxicity [15]. As the largest immune system compartment, the intestine is increasingly recognized for its role in disease progression [16], and numerous studies have examined ZEN's

Peer review under responsibility of Xi'an Jiaotong University

* Corresponding author.

** Corresponding author.

E-mail addresses: jyluo@implad.ac.cn (J. Luo), yangmeihua15@hotmail.com (M. Yang).

impact on intestinal immunotoxicity. Recent research using mouse spleen lymphocytes exposed to ZEN (10 and 20 μM , 72 h) revealed immunosuppression through the inhibition of CD4^+ T cell activation [17]. Proteomic analyses conducted on an *in vitro* culture model of pig jejunal explants exposed to ZEN (100 μM , 4 h) demonstrated that ZEN affected immune function in the pig intestine, with observed alterations linked to carcinogenesis [18]. Furthermore, ZEN was found to exert immunosuppressive effects on the intestine of grass carp through dietary exposure to varying levels of ZEN (0–2,507 $\mu\text{g}/\text{kg}$ diet) for 70 days [19].

The potential associations between exposure to mycotoxins and diseases of unknown origin have been largely overlooked [20]. Currently, the link between aflatoxin B1 exposure and liver cancer is well-established [21], while the carcinogenicity of other mycotoxins is under extensive investigation [22]. Several case reports have indicated a strong correlation between inhalation exposure to mycotoxins and Alzheimer's disease (AD) [23]. Additionally, Payros et al. [24] discovered an increased risk of inflammatory bowel disease due to deoxynivalenol exposure. The use of bioinformatics analysis has been widespread in identifying potential connections between external exposures and diseases [25].

Our study revealed significant alterations in the expression levels of the apolipoprotein E (ApoE) protein in the intestine of rats exposed to ZEN. ApoE, as one of the crucial apolipoproteins in the human body, plays a key role in lipid accumulation, transport, secretion, and metabolism [26]. It is closely associated with cell proliferation, metabolism, and immune status [27]. There is substantial evidence supporting the notion that ApoE dysfunction is a major risk factor for AD [28], atherosclerosis [29], hyperlipidemia [30], and other diseases.

Emerging evidence suggests a close relationship between innate immune responses and lipid metabolism [31]. Given that the mechanisms underlying ZEN-induced intestinal immunosuppression remain unclear, we aimed to investigate the potential involvement of lipid metabolism imbalance. Gaining a better understanding of the mechanistic effects of ZEN could contribute to the identification of preventive and therapeutic strategies for ZEN-induced immunotoxicity. Furthermore, we conducted a bioinformatic analysis combining our experimental results with the latest cancer gene database to explore the connection between ZEN exposure and cancer. These findings provide a theoretical foundation for further regulations on ZEN in food and feed products.

2. Materials and methods

2.1. Chemicals and reagents

ZEN and lipopolysaccharide (LPS) were obtained from Yuanye Co., Ltd. (Shanghai, China). Liver X receptor (LXR)-623 and a peptide fragment of ApoE and an $\alpha 7$ nAChR antagonist (C₉₇H₁₈₁N₃₇O₁₉, COG-133) were obtained from GlpBio Co., Ltd. (Montclair, CA, USA). Roswell Park Memorial Institute (RPMI)-1640 culture medium, penicillin/streptomycin (100 \times), and fetal bovine serum (FBS) were obtained from Corning Inc. (New York City, NY, USA). Detailed information regarding the antibodies is shown in Section S1.1 in the Supplementary data.

2.2. Animal study

The animal study was conducted in accordance with a standardized protocol and received approval from the Laboratory Animal Center, Institute of Medicinal Plant Development, Chinese Academy of Medical Sciences & Peking Union Medical College, Beijing, China (Approval No.: SLXD-20210422017). The study adhered to the guidelines outlined in the Guide for the Care and Use

of Laboratory Animals published by the US National Institutes of Health and the Animal Research: Reporting of *In Vivo* Experiments (ARRIVE) guidelines. Sprague–Dawley (SD) rats were randomly divided into two groups: a control group ($n = 10$) and a ZEN group ($n = 10$). The ZEN group received ZEN at a dosage of 5 mg/kg/day b.w., dissolved in 0.3% sodium carboxymethyl cellulose, administered via gavage for a period of 14 days. The control group received an equivalent volume of vehicle (0.3% sodium carboxymethyl cellulose) to match the ZEN group. The chosen dosage was based on a previous animal study that demonstrated ZEN-induced changes in intestinal barrier functions in SD rats using a dosage of 5 mg/kg/day b.w [32]. Further details regarding the animal study procedure is shown in Section S2.1 in the Supplementary data.

2.3. Hematoxylin and eosin (HE) staining

HE staining was conducted according to a previously described method [33] using a standardized protocol. Detailed descriptions of the HE staining procedure is shown in Section S2.2 in the Supplementary data.

2.4. Immunohistochemical (IHC) staining

IHC staining was conducted using a standardized protocol, following the previously described method [34]. Detailed explanations of the IHC staining procedure is shown in Section S2.3 in the Supplementary data.

2.5. Immunofluorescence (IF) staining

IF staining was carried out using a standardized protocol, following the previously described method [35]. Detailed descriptions of the IF staining procedure is shown in Section S2.4 in the Supplementary data.

2.6. Western blot

Western blot analysis was conducted using a standardized protocol, following the previously described method [36]. Detailed descriptions of the Western blot procedure is shown in Section S2.5 in the Supplementary data.

2.7. Metabolomic analysis of rat serum

Rat serum metabolites were assayed and analyzed using previously described methods [37], following standard operating procedures. Detailed descriptions of the procedure is shown in Section S2.6 in the Supplementary data.

2.8. Proteomic analysis of rat intestine

Proteomic analysis of rat intestine was conducted and analyzed using previously described methods [38], following standard operating procedures. Detailed descriptions of the procedure is shown in Section S2.7 in the Supplementary data.

2.9. Rat 27-hydroxycholesterol (27-HC) enzyme-linked immunospecific assay (ELISA)

A rat 27-HC ELISA was conducted following a standardized protocol, as previously described [39]. Detailed descriptions of the procedure is shown in Section S2.8 in the Supplementary data.

2.10. Rat spleen lymphocyte suspension preparation

Ten female SD rats were euthanized using an intraperitoneal injection of urethane (20%, 1 g/kg). The spleen was then collected, gently ground, and prepared as a single-cell suspension. Rat spleen lymphocytes were isolated following the standard procedure of a rat spleen lymphocyte isolation medium kit [40]. Detailed descriptions of the procedure for preparing the rat spleen lymphocyte suspension is shown in Section S2.9 in the Supplementary data.

2.11. Cell culture

Rat spleen lymphocytes were cultured under routine conditions in RPMI-1640 supplemented with 10% FBS and 1% penicillin/streptomycin at 37 °C, pH 7.4, in a 5% CO₂ atmosphere. A total of 3 × 10⁶ cells/mL were plated in 6-well plates, and the groups were categorized based on the following compound administration methods: 1) control group: RPMI-1640 only; 2) LPS group: LPS (0.5 µg/mL) dissolved in RPMI-1640; 3) ZEN low-dose group: LPS (0.5 µg/mL) + ZEN (5 µM) dissolved in RPMI-1640 containing 0.005% methanol; 4) ZEN high-dose group: LPS (0.5 µg/mL) + ZEN (10 µM) dissolved in RPMI-1640 containing 0.01% methanol; 5) COG-133 (ApoE agonist) group: LPS (0.5 µg/mL) + ZEN (10 µM) + COG-133 (10 µM) dissolved in RPMI-1640 containing 0.01% methanol; and 6) LXR-623 (LXR agonist) group: LPS (0.5 µg/mL) + ZEN (10 µM) + LXR-623 (4 µM) dissolved in RPMI-1640 containing 0.01% dimethyl sulfoxide (DMSO). Detailed descriptions of how compounds were administered to the cells is shown in Section S2.10 in the Supplementary data.

2.12. Flow cytometry

Flow cytometry was conducted following a standardized protocol, as previously described [41]. Detailed descriptions of the flow cytometry procedure is shown in Section S2.11 in the Supplementary data.

2.13. Bioinformatics analysis

Bioinformatics analysis was conducted following a standardized protocol, as previously described. To assess *ApoE* gene expression differences between tumors and adjacent normal tissues of various tumor types or subtypes from the The Cancer Genome Atlas (TCGA) dataset, the “Gene-DE” module of tumor immune estimation resource (TIMER2, version 2, <http://timer.cistrome.org/>) was utilized. In addition, UALCAN’s “individual cancer stages” module (<http://ualcan.path.uab.edu/analysis-prot.html>) was used to generate *ApoE* expression box plots for low-*ApoE*-expressing TCGA tumors in different pathological stages (stages I, II, III, and IV). Protein expression analysis was performed using the Clinical Proteomic Tumor Analysis Consortium (CPTAC) dataset in UALCAN. Detailed descriptions of the bioinformatics analysis procedure is shown in Section S2.12 in the Supplementary data [42–51].

2.14. Statistical analyses

Statistical analyses were conducted using GraphPad Prism 8.0.2 statistical software. Replicate measurements were obtained from distinct biological samples. The data are presented as mean ± standard deviation (SD). Student’s *t*-test was employed for all statistical analyses. Probability values with $P < 0.05$ are considered statistically significant, while probability values with $P < 0.01$ are considered extremely significant. Kaplan-Meier (K-M) plots were generated with *P*-values obtained from a log-rank test. Gene expression correlations were assessed using Spearman’s correlation. Receiver operating

characteristic (ROC) curves were plotted using the “survival-ROC” package in R. Cell clustering was performed using the FindClusters function implemented in the Seurat R package.

3. Results

3.1. ZEN induces intestinal immunosuppression by inhibiting T lymphocyte activation

To investigate the effects of ZEN on the intestine, we administered ZEN (5 mg/kg/day) to rats. Compared to the control group, rats in the ZEN group exhibited a significant reduction in body weight (Fig. 1A). HE staining revealed dilatation of the intestinal lumen, incomplete villus structure, mucosal erosion, and epithelial cell loss due to ZEN exposure (Fig. 1B). Additionally, the levels of tumor necrosis factor- α (TNF- α) and interferon- γ (IFN- γ), which activate the innate immune response, were significantly decreased in the ZEN group compared to the control group (Fig. 1C) ($P < 0.05$). On the other hand, the levels of interleukin-10 (IL-10), transforming growth factor- β (TGF- β), and arginase-1 (Arg-1), which limit the innate immune response, were significantly higher in the ZEN group than in the control group ($P < 0.01$ and $P < 0.05$) (Fig. 1D).

Previous studies have demonstrated the interference of ZEN with mouse T lymphocyte activation [52]. To assess the impact of ZEN on T lymphocytes in the rat intestine, we measured the levels of CD3, CD4, and CD8. IHC results showed that CD3 levels were significantly reduced in the ZEN group compared to the control group ($P < 0.05$) (Fig. 1E). Furthermore, Western blot analysis revealed a significant decrease in CD4 and CD8 levels in the ZEN group ($P < 0.05$) (Fig. 1F). These findings suggest that ZEN may induce immunosuppression in the rat intestine by inhibiting T lymphocyte activation.

3.2. ZEN causes blood lipid metabolism disturbances

To gain further insights into the role of metabolic alterations in ZEN-induced immunosuppression, we conducted metabolomics analysis to investigate the effects of ZEN exposure on rat serum metabolites. Principal component analysis (PCA) was performed on the metabolome to visualize the overall metabolic profiles (Fig. 2A), and orthogonal partial least squares discrimination analysis (OPLS-DA) was employed to differentiate metabolic profiles between the control group and ZEN group ($R^2X = 0.467$, $R^2Y = 0.996$, $Q^2 = 0.729$; Figs. 2B and S1). By integrating log₂(fold change) and variable importance in projection (VIP), we identified 78 altered metabolites in ZEN-exposed rat serum, including 25 downregulated and 53 upregulated metabolites (Fig. 2C). The cluster heatmap revealed that the upregulated metabolites primarily belonged to organic acids and their derivatives, amino acids and their metabolites, and bile acids, while the downregulated metabolites mainly consisted of fatty acids, hormones and hormone-related compounds, and glycerophospholipids (Figs. 2D and S2 and Table S1).

Based on a significance threshold of $P < 0.05$, we further selected differentially expressed metabolites (DEMs) by combining the top-ranked metabolites derived from VIP (Fig. 2E) and log₂(fold change) (Fig. 2F). Among the identified DEMs, the most prominent upregulated metabolites in the ZEN group (Fig. 2G) were bile acids, such as 7-ketodeoxycholic acid and α -muricholic acid ($P < 0.05$ and $P < 0.01$) (Fig. 2H). Notably downregulated DEMs in the ZEN group included ω -3 unsaturated fatty acids, such as eicosapentaenoic acid and 14(*S*)-hydrocosahexaenoic acid (HDHA) ($P < 0.05$), lysophosphatidylcholine, such as lysophosphatidylcholine (LPC) (20:5/0:0) and lysophosphatidic acid (LPA) (0:0/18:0) ($P < 0.01$), carnitine, such as carnitine C8:1 and carnitine C16:3 ($P < 0.01$), free fatty acids, such as γ -linolenic acid (C18:3) and docosahexaenoic acid

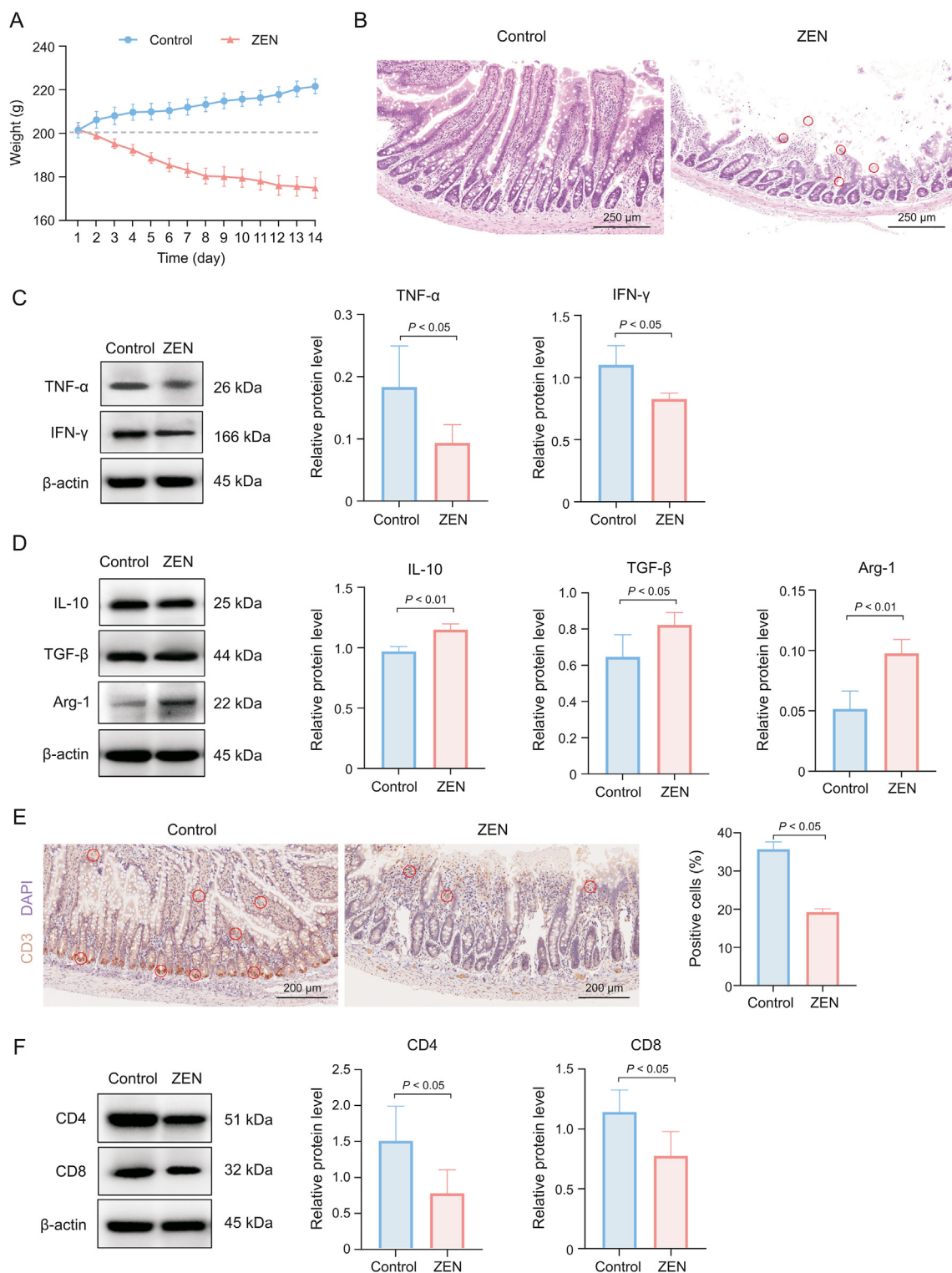


Fig. 1. Zearalenone (ZEN) administration induces immunotoxicity in rat intestine. (A) Changes in body weight of rats in control and ZEN groups after 14 days of administration. (B) Representative images of hematoxylin and eosin (HE) staining (100×) of intestine in control and ZEN groups. (C) Protein levels of tumor necrosis factor-α (TNF-α) and interferon-γ (IFN-γ) in rat intestine of control and ZEN groups. (D) Protein levels of interleukin-10 (IL-10), transforming growth factor-β (TGF-β), and arginase-1 (Arg-1) in rat intestine of control and ZEN groups. (E) Representative images of immunohistochemistry staining (100×) of CD3 positive cells and proportion of CD3 positive cells in rat intestine of control and ZEN groups. (F) Protein levels of CD4 and CD8 in rat intestine of control and ZEN groups (n = 3). The data are presented as mean ± standard deviation (SD). Student's *t*-test was employed for all statistical analyses. Probability values with *P* < 0.05 are considered statistically significant, while probability values with *P* < 0.01 are considered extremely significant. DAPI: 4',6-diamidino-2-phenylindole.

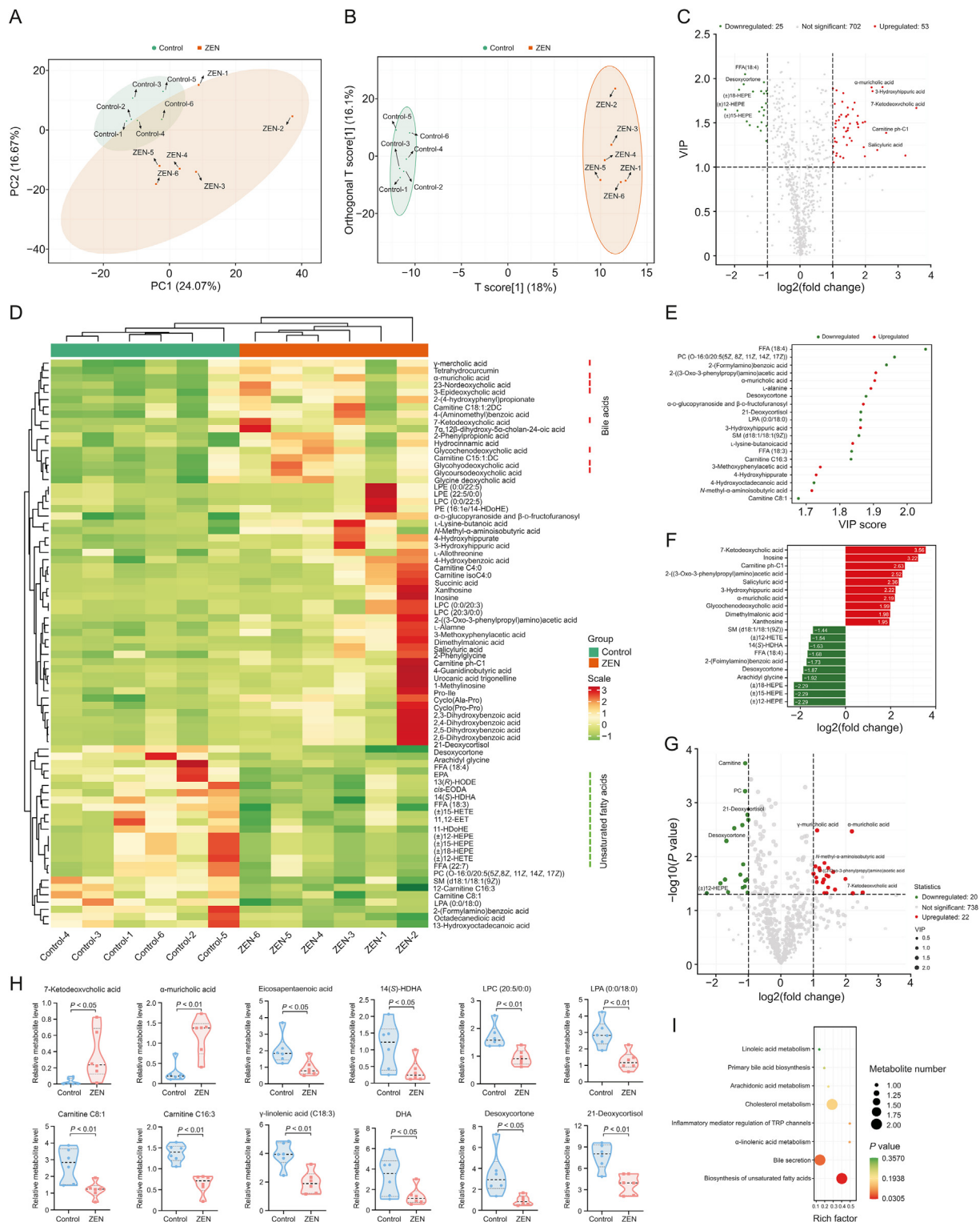


Fig. 2. Metabolomics analysis of rat serum after zearalenone (ZEN) administration. (A) Principal component analysis (PCA) of the metabolome to intuitively showed the differences between samples from control and ZEN groups as indicated. (B) Orthogonal partial least squares discrimination analysis (OPLS-DA) showed the possible discrimination of metabolites in serum from control and ZEN groups as indicated. (C) The volcano plot of differentially expressed metabolites (DEMs) between control and ZEN groups. (D) Clustering heatmap of the DEMs between control and ZEN groups. (E) Variable importance in projection (VIP) score plot of Top 20 DEMs between control and ZEN groups. (F) log₂(fold change) bar chart of Top 20 DEMs between control and ZEN groups. (G) The volcano plot of DEMs between control and ZEN groups. (H) Violin plots of representative DEMs between control and ZEN groups. (I) Kyoto Encyclopedia of Genes and Genomes (KEGG) pathway analysis of DEMs between control and ZEN groups (n = 6). The data are presented as mean ± standard deviation (SD). Student's t-test was employed for all statistical analyses. Probability values with P < 0.05 are considered statistically significant, while probability values with P < 0.01 are considered extremely significant. FFA: free fatty acid; HEPE: 5-hydroxyeicosapentaenoic acid; DC: deoxycytidine; LPE: lysophosphatidyl ethanolamine; LPC: lysophosphatidylcholine; PE: phosphatidyl ethanolamine; HDoHE: 14-hydroxyeicosapentaenoic acid; EPA: eicosapentaenoic acid; HODE: hydroxyoctadecadienoic acid; EODA: epoxyoctadecanoic acid; HDHA: hycosahexaenoic acid; HETE: hydroxyeicosatetraenoic acid; EET: epoxyeicosatrienoic acid; PC: phosphatidylcholine; SM: sphingomyelin; LPA: lysophosphatidic acid; DHA: docosahexaenoic acid; TRP: tryptophan.

($P < 0.01$ and $P < 0.05$), and sterols, such as desoxycortone and 21-deoxycortisol ($P < 0.05$ and $P < 0.01$) (Fig. 2H). Moreover, DEM correlation analysis revealed significant associations among lipid compounds, including fatty acids, bile acids, hormones, and hormone-related components (Fig. S3). Kyoto Encyclopedia of Genes and Genomes (KEGG) analysis of the DEMs (Fig. 2I) indicated that ZEN exposure disrupted lipid metabolism pathways, particularly primary bile acid biosynthesis, unsaturated fatty acid biosynthesis, and cholesterol metabolism pathways, by elevating bile acid levels and reducing unsaturated fatty acid levels, thereby leading to disturbances in lipid metabolism.

3.3. ZEN induces lipid abnormalities in rat intestine

ZEN exposure had a systemic impact on lipid metabolism, as evident from the analysis of rat serum. To investigate the specific effects of ZEN on the rat intestine, we conducted proteomic analyses. OPLS-DA was employed to differentiate proteomes between the control group and the ZEN group ($R^2X = 0.719$, $R^2Y = 0.999$, and

$Q^2 = 0.557$; Figs. 3A and S4). By integrating $\log_2(\text{fold change})$ and P -values, we identified 22 altered proteins (11 downregulated and 11 upregulated) in ZEN-exposed rat intestine (Fig. 3B). Cluster heatmap analysis was performed using the differentially expressed proteins (DEPs) (Table S2 and Fig. 3C).

Clusters of Orthologous Groups (COG) and Gene Ontology (GO) protein classification analyses indicated that the functions of the DEPs were primarily associated with lipid transport and metabolism, as well as transporter activity structure (Figs. S5A and B). Notably, extracellular proteins accounted for 40.91% of the DEPs (Fig. S5C). GO enrichment analysis of the DEPs revealed that ZEN exposure affected metabolic pathways in the rat intestine, including lipid metabolism and regulation of cholesterol metabolic processes. Additionally, ZEN activated pathways associated with the response to toxic substances (Fig. 3D). Furthermore, biological process enrichment analysis identified the impact of ZEN exposure on sterol and steroid synthesis and metabolism in the rat intestine (Fig. 3E).

To further investigate the key targets of ZEN-induced intestinal immunotoxicity in rats, we intersected the DEPs with key

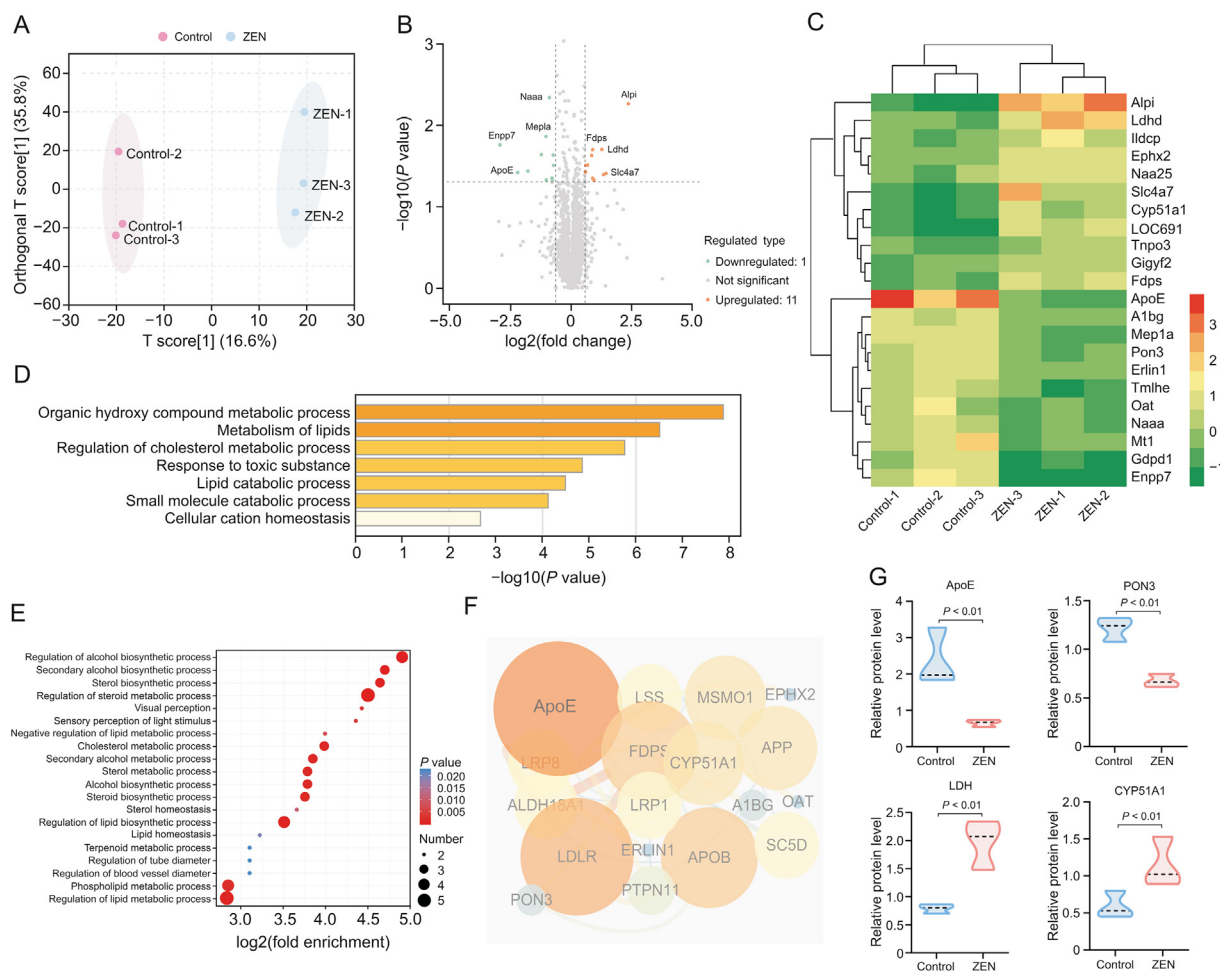


Fig. 3. Proteomic analysis of rat intestine after zearalenone (ZEN) administration. (A) Orthogonal partial least squares discrimination analysis (OPLS-DA) showed the possible discrimination of proteins in intestine from control and ZEN groups as indicated. (B) The volcano plot of differentially expressed proteins (DEPs) between control and ZEN groups. (C) Clustering heatmap of the DEPs between control and ZEN groups. (D) The Gene Ontology (GO) analysis of DEPs between control and ZEN groups. (E) The biological process enrichment analysis of DEPs between control and ZEN groups. (F) The protein-protein interaction (PPI) network analysis of intersection of DEPs and immunotoxic targets. (G) Violin plots of representative DEPs between control and ZEN groups ($n = 3$). The data are presented as mean \pm standard deviation (SD). Student's t -test was employed for all statistical analyses. Probability values with $P < 0.05$ are considered statistically significant, while probability values with $P < 0.01$ are considered extremely significant. ApoE: apolipoprotein E; LSS: lanosterol synthase; MSMO1: methylsterol monooxygenase 1; EPHX2: bifunctional epoxide hydrolase 2; LRP8: low-density lipoprotein receptor-related protein 8; FDPS: farnesyl pyrophosphate synthase; CYP51A1: lanosterol 14- α demethylase; APP: amyloid- β precursor protein; ALDH18A1: delta-1-pyrroline-5-carboxylate synthase; LRP1: prolow-density lipoprotein receptor-related protein 1; A1BG: alpha-1B-glycoprotein; OAT: ornithine-delta-aminotransferase; LDLR: low-density lipoprotein receptor; ERLIN1: endoplasmic reticulum lipid raft-associated protein 1; APOB: apolipoprotein B; SC5D: lathosterol oxidase; PON3: serum paraoxonase/lactonase 3; PTPN11: tyrosine-protein phosphatase non-receptor type 11; LDH: lactate dehydrogenase.

immunotoxicity targets and screened for overlapping targets. Protein-protein interaction network analysis revealed the involvement of proteins such as ApoE, lactate dehydrogenase (LDH), lanosterol 14- α demethylase (CYP51a1), and serum paraoxonase/lactonase 3 (Pon3) (Figs. 3F and G) in ZEN-induced intestinal immunotoxicity. Notably, among the DEPs in the control vs. ZEN comparison, ApoE exhibited the highest fold change (FC) value. Therefore, we consider ApoE to play a crucial role in the ZEN-induced intestinal toxicity in rats.

3.4. ZEN downregulates 27-HC level, inhibits LXR/ApoE activation, and promotes MDSCs proliferation

Lipid metabolism plays a critical role in regulating T cell responses. To investigate the impact of ZEN-induced disruption of lipid metabolism on T cell immunity, we identified key targets associated with abnormal lipid metabolism by combining serum metabolomic analysis and intestinal proteomic analysis in rats. Among the identified targets, ApoE stood out as a protein of interest. ApoE is involved in lipid transport and plays a crucial role in lipid metabolism. Consequently, we assessed ApoE protein levels in the rat intestine using IF staining and Western blot. The IF staining revealed a significant reduction in ApoE levels in the ZEN group compared to the control group (Fig. 4A). Similarly, the Western blot results demonstrated that ZEN exposure significantly inhibited ApoE expression in the rat intestine ($P < 0.01$) (Fig. 4B).

LXR α and β are transcriptional regulators of cholesterol, fatty acid, and phospholipid metabolism and serve as upstream regulators of ApoE [53]. Previous studies by Tavazoei et al. [54] demonstrated the involvement of the LXR/ApoE axis in regulating innate immune suppression, where downregulation of ApoE promotes the proliferation of circulating myeloid-derived suppressor cells (MDSCs), leading to the inhibition of T lymphocyte activation. Based on this knowledge, we speculated that the immunosuppressive effect of ZEN on T lymphocytes might be associated with the LXR/ApoE/MDSCs axis. To explore this further, we examined the levels of LXRs and MDSCs markers in the rat intestine using Western blot. Compared to the control group, both LXR α and β were significantly downregulated in the ZEN group ($P < 0.05$ and $P < 0.01$) (Fig. 4C), with LXR β exhibiting a greater FC (FC = 4.46) than LXR α (FC = 1.79). Gr-1 and CD11b are widely utilized as markers for detecting MDSCs and assessing their proliferation [55]. Our experimental results demonstrated significantly higher levels of Gr-1 and CD11b in the rat intestine of the ZEN group compared to the control group ($P < 0.01$ and $P < 0.05$) (Fig. 4D), indicating that ZEN exposure promoted MDSCs proliferation.

Proteomic analysis revealed that ZEN exposure affected sterol and steroid synthesis and metabolism (Fig. 3E). LXR transcriptional activity is regulated by oxysterols, oxidized forms of cholesterol. Among these, 27-HC is a major endogenous oxysterol that has drawn interest in the fields of lipid metabolism and immunology as an LXR agonist [56]. LXR agonists, including 27-HC, have been shown to inhibit MDSCs proliferation by activating LXRs/ApoE, thereby promoting T lymphocyte activation [57]. Therefore, we measured the levels of 27-HC in the rat intestine using ELISA and found that it was significantly downregulated in the ZEN group compared to the control group ($P < 0.01$) (Fig. 4E). These findings suggest that ZEN suppresses T lymphocytes by downregulating 27-HC, which inhibits LXRs/ApoE and promotes MDSCs proliferation in the rat intestine.

3.5. ApoE or LXR agonists alleviate ZEN's inhibitory effect on T lymphocyte activation

To validate the involvement of LXRs/ApoE in ZEN-induced immunosuppression, we utilized a rat spleen lymphocyte model.

In this model, we first activated T lymphocytes by administering LPS and then inhibited T lymphocyte proliferation through ZEN exposure. Subsequently, we investigated the impact of ApoE or LXR agonists (COG-133 or LXR-623) [58,59] on ZEN-induced T lymphocyte immunosuppression using flow cytometry.

Our findings revealed significantly lower levels of CD3⁺ lymphocytes (T lymphocytes) in the ZEN groups ($P < 0.01$) compared to the LPS group (Fig. 5A), indicating that ZEN exposure hindered T lymphocyte activation. Further experiments demonstrated that ZEN exposure concurrently suppressed the activation of CD3⁺CD4⁺ lymphocytes (helper T lymphocytes (Th cells)) ($P < 0.01$) (Fig. 5B) and CD3⁺CD8⁺ lymphocytes (cytotoxic T lymphocytes (CTLs)) ($P < 0.01$) (Fig. 5C).

Comparatively, treatment with ApoE or LXR agonists exhibited a significant alleviation of ZEN-induced inhibition on Th cells ($P < 0.01$) (Fig. 5B) and CTLs ($P < 0.01$) (Fig. 5C) when compared to the ZEN high-dose group. These results strongly suggest that LXR/ApoE inhibition is a critical mechanism underlying ZEN-induced immunotoxicity (Fig. 6).

3.6. The ApoE gene is significantly downregulated in colon adenocarcinoma and other specified cancers

Our experimental findings provide evidence that ZEN exposure significantly reduces the expression of ApoE in tissues by affecting serum metabolites, leading to immunosuppression through ApoE downregulation. Immunosuppression is closely linked to the occurrence and progression of cancer. ZEN, recognized as a carcinogen by the World Health Organization (WHO), has been extensively studied for its mutagenic and carcinogenic effects. A systematic review has suggested a potential association between ZEN and its metabolites and an increased risk of breast cancer [60]. Moreover, recent research has indicated that ZEN promotes the advancement of colon cancer by enhancing the BEST4/AKT/ERK1/2 pathway [61]. However, the precise carcinogenic mechanism of ZEN and the relationship between low ApoE expression and cancer remain unclear. Therefore, we conducted a pan-cancer analysis of ApoE to explore the possible connection between ZEN-induced downregulation of ApoE and the occurrence and development of cancer, providing insights for future cancer research involving ZEN.

In our analysis of the TCGA dataset, we performed a differential expression analysis of the ApoE gene in tumors. We observed significant abnormal expression of the ApoE gene in 16 normal and tumor cancer tissues among 34 different cancers (Fig. 7A). Notably, the ApoE gene exhibited significant downregulation in tumor tissues of seven cancers compared to normal tissues, including adrenocortical carcinoma (ACC) ($P < 0.01$), cholangiocarcinoma (CHOL) ($P < 0.01$), acute myeloid leukemia (LAML) ($P < 0.01$), lung squamous cell carcinoma (LUSC) ($P = 0.03$), colon adenocarcinoma (COAD) ($P = 0.02$), rectum adenocarcinoma (READ) ($P = 0.03$), and ovarian serous cystadenocarcinoma (OV) ($P < 0.01$) (Fig. 7B). Furthermore, the UALCAN "individual cancer stages" module analysis revealed that the downregulation of the ApoE gene in CHOL, COAD, and lung adenocarcinoma (LUAD) was associated with pathological cancer stage (Fig. 7C).

3.7. ApoE protein is significantly downregulated in colon adenocarcinoma and other specified cancers

The analysis of the CPTAC dataset (Fig. 8A) revealed lower expression of ApoE total protein in breast cancer, renal cell carcinoma (RCC), head and neck squamous cell carcinoma (HNSC), uterine corpus endometrial carcinoma (UCEC), ovarian cancer, colon

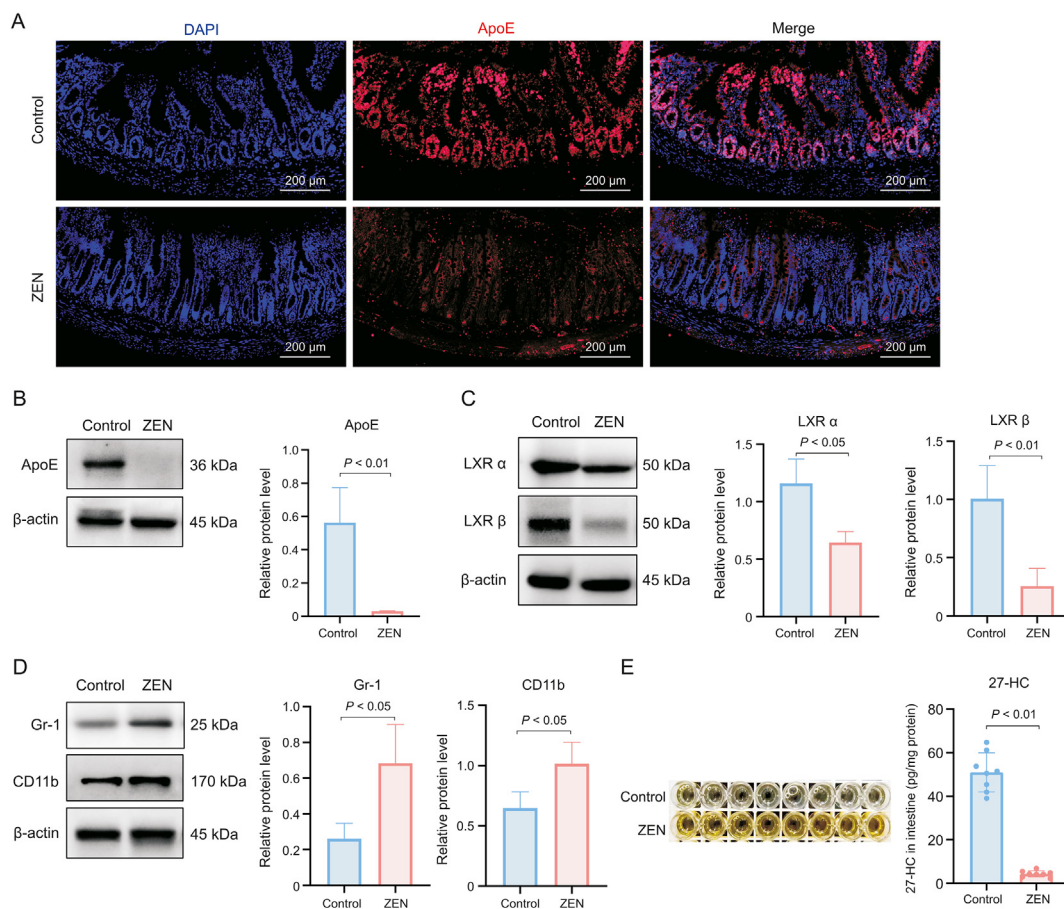


Fig. 4. Zearalenone (ZEN) exerts immunotoxicity by interfering with the liver X receptor (LXR)/apolipoprotein E (ApoE)/myeloid-derived suppressor cells (MDSCs) by down-regulating 27-hydroxycholesterol (27-HC) levels. (A) Representative images of immunofluorescence staining (100 \times) of ApoE positive cells in control and ZEN groups. (B) Protein level of ApoE in control and ZEN groups. (C) Protein level of LXR α and LXR β in control and ZEN groups. (D) Protein levels of CD11b and Gr-1 in control and ZEN groups. (E) Enzyme-linked immunospecific assay (ELISA) of 27-HC levels in control and ZEN groups ($n = 3$). The data are presented as mean \pm standard deviation (SD). Student's t -test was employed for all statistical analyses. Probability values with $P < 0.05$ are considered statistically significant, while probability values with $P < 0.01$ are considered extremely significant. DAPI: 4',6-diamidino-2-phenylindole.

cancer, and LUAD primary tissues compared to normal tissues ($P < 0.01$) (Fig. 8B). Additionally, the UALCAN “individual cancer stages” module analysis indicated that the downregulation of ApoE protein in breast cancer, RCC, HNSC, ovarian cancer, colon cancer, and LUAD was correlated with the pathological cancer stage (Fig. 8C).

Considering the significant downregulation of ApoE gene or protein levels in tumor tissues based on the TCGA and CPTAC databases, as well as the correlation between ApoE expression and tumor pathological stage, we selected tumors with low ApoE expression that exhibited significant differences and strong correlations for further in-depth analysis. These tumors included breast cancer, colorectal cancer (COAD and READ), and lung cancer (LUSC and LUAD).

3.8. Low ApoE gene expression is significantly associated with poor overall survival (OS) prognosis in LUAD patients

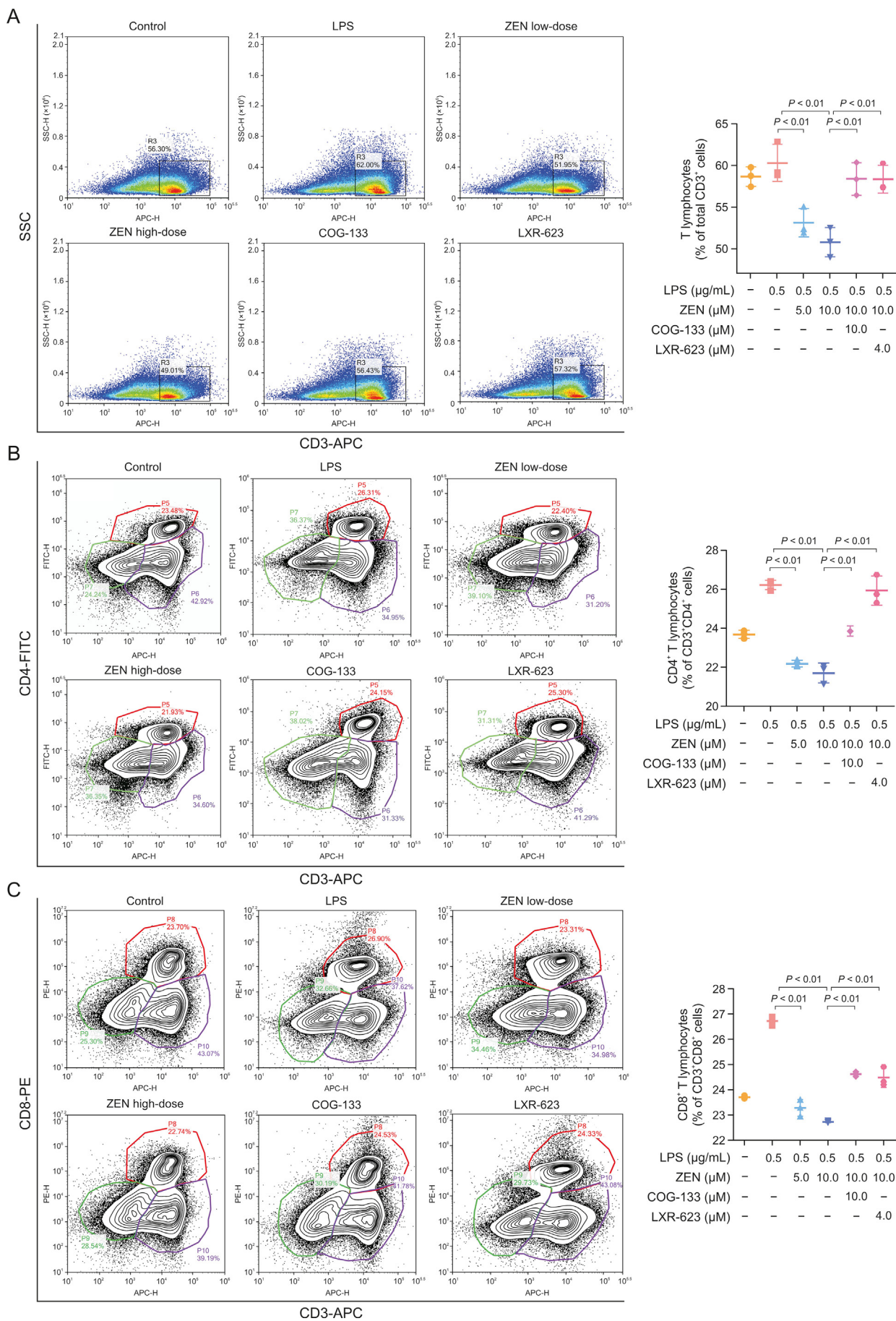
Based on our survival analysis, we found that low ApoE expression was not correlated with poor prognosis in breast invasive carcinoma (BRCA) overall (Fig. S6A) ($P = 0.93$). However, it was significantly associated with poor prognosis in postmenopausal BRCA patients ($P = 0.017$) (Fig. S6A). Furthermore, low ApoE expression did not correlate with poor OS prognosis in READ ($P = 0.44$) (Fig. S6B). On the other hand, we observed a significant association between low ApoE expression and poor OS prognosis in LUAD patients ($P = 0.038$) (Fig. S6C).

3.9. Uterine carcinosarcoma (UCS) cases with altered ApoE showed poor survival prognosis

We analyzed various tumors in the TCGA database to assess ApoE genetic alterations and discovered that the most frequent alteration (>8%) occurred in patients with UCS categorized as “amplification” (Fig. S7A). These genetic alterations primarily manifested as ApoE missense mutations. Specifically, we identified the K87N alteration within the apolipoprotein A1/A4/E domain, which was observed in two cases of skin cutaneous melanoma and led to a frame shift mutation in the ApoE gene (Fig. S7B). We also visualized the 3D structure of the ApoE protein with the K87N site alteration (Fig. S7C). Among UCS patients with altered ApoE, the overall clinical prognosis was notably poor ($P < 0.01$), with lower disease-specific survival ($P < 0.01$) and progression-free survival ($P < 0.01$) compared to cases without ApoE alteration (Fig. S7D). This finding warrants further investigation.

3.10. The ApoE gene is positively correlated with DNA methylation in colorectal and lung cancer

We conducted an analysis using the TCGA database to explore the relationship between ApoE DNA methylation and breast, colorectal, and lung cancers. The correlation analysis between ApoE and cg08955609 (Fig. 9A) revealed a weak or non-existent



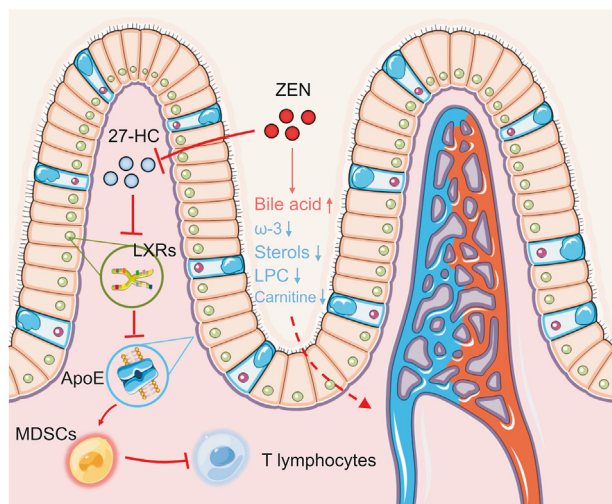


Fig. 6. Toxic mechanism of zearalenone (ZEN) induced intestinal immunosuppression: ZEN promotes myeloid-derived suppressor cells (MDSCs) proliferation by disrupting the 27-hydroxycholesterol (27-HC)/liver X receptor (LXR)/apolipoprotein E (ApoE) axis, thereby inhibiting T lymphocyte activation in the rat intestine. LPC: lysophosphatidylcholine.

correlation in BRCA ($r = 0.114$) ($P < 0.01$). On the other hand, the correlation analysis between *ApoE* and cg01032398 (Fig. 9A) demonstrated a positive correlation between *ApoE* expression and DNA methylation in COAD ($r = 0.367$) ($P < 0.01$), READ ($r = 0.316$) ($P < 0.01$), LUAD ($r = 0.326$) ($P < 0.01$), and LUSC ($r = 0.394$) ($P < 0.01$). These findings suggest that DNA methylation of the *ApoE* gene may be associated with the development of colorectal and lung cancers.

3.11. *ApoE* is significantly negatively correlated with MDSCs immune infiltration in breast, colorectal, and lung cancer

Our experimental findings demonstrated that exposure to ZEN resulted in the downregulation of *ApoE*, which in turn promoted the proliferation of MDSCs in the rat intestine. To investigate the impact of *ApoE* on MDSCs in cancer patients, we utilized the TCGA database to analyze the relationship between *ApoE* gene expression and MDSCs infiltration levels in breast cancer, colorectal cancer, and lung cancer tumor samples. The results revealed a significant negative correlation between *ApoE* expression and MDSCs immune infiltration (Fig. 9B) in BRCA ($r = -0.327$) ($P < 0.01$), BRCA-Her2 ($r = -0.511$) ($P < 0.01$), COAD ($r = -0.506$) ($P < 0.01$), READ ($r = -0.429$) ($P < 0.01$), LUAD ($r = -0.38$) ($P < 0.01$), and LUSC ($r = -0.605$) ($P < 0.01$). These correlation analyses between *ApoE* expression and MDSCs immune infiltration in clinical tumor samples are consistent with our experimental findings.

3.12. *ApoE* is significantly positively correlated with LXR in breast, colorectal, and lung cancer

Our experimental findings demonstrated that exposure to ZEN in the rat intestine resulted in the downregulation of *ApoE* expression through the inhibition of LXR. To further investigate the relationship between *ApoE* and LXR expression in cancer

patients, we examined the correlation between their expression levels in breast cancer, colorectal cancer, and lung cancer tumor samples obtained from the TCGA database. The results revealed a significant positive correlation between *ApoE* and LXR expression (Fig. 10) in BRCA ($R = 0.538$) ($P < 0.01$), COAD/READ ($R = 0.455$) ($P < 0.01$), COAD ($R = 0.503$) ($P < 0.01$), LUAD ($R = 0.562$) ($P < 0.01$), and LUSC ($R = 0.702$) ($P < 0.01$). These findings are consistent with our experimental results, indicating that *ApoE* expression levels and LXR levels are correlated in clinical tumor samples.

3.13. Certain immune cell lineages downregulate *ApoE* in colorectal cancer

To further investigate the potential association between ZEN-induced *ApoE* downregulation and colorectal cancer risk, we conducted a single-cell analysis to examine *ApoE* expression and distribution in both normal tissue and colorectal cancer clinical samples. This study included seven samples obtained from three colorectal cancer patients, resulting in the analysis of 14,526 cells from normal tissues and 15,464 cells from tumor tissues (Fig. S8A). After eliminating batch effects, regressing out unique molecular identifiers (UMIs) and mitochondrion-derived UMIs counts, and applying quality filtering, a total of 25,650 cells with at least 200 UMIs were included in the analysis (Fig. S8B).

Surprisingly, *ApoE* emerged as one of the top 10 magnet genes with a significant fold difference, making it suitable for clustering and cell identification purposes (Fig. S8C). This highlights the crucial role of *ApoE* in the pathogenesis and progression of colorectal cancer. By screening for effective PCs (Fig. S8D), we divided the cells into 25 major cell lineages, which comprised nine immune cell lineages ($CD45^+$), including natural killer cells, T helper cells, T cells, B cells, NKT cells, $CD4^+$ T cells, $CD1C^+$ -B dendritic cells, plasma cells, and mast cells, as well as ten non-immune cell lineages ($CD45^-$), including $LGR5^+$ stem cells, neural progenitor cells, trophoblast cells, goblet cells, sertoli cells, $DCLK1^+$ progenitor cells, intestinal glial cells, cancer stem cells, paneth cells, intestinal epithelial cells, and $MKI67^+$ progenitor cells (Figs. 11A and B).

Analysis of *ApoE* gene expression revealed a significant downregulation in tumor tissues compared to normal tissues in B cells, $CD4^+$ T cells, $CD1C^+$ -B dendritic cells, plasma cells, neural progenitor cells, and paneth cells (Fig. 11C). Furthermore, the immune cell lineage scale histogram demonstrated significantly lower levels of T cells and NK cells in colorectal cancer tissue samples compared to normal tissue samples (Fig. 11D). These findings suggest a potential link between the observed T cell suppression and *ApoE* downregulation in colorectal cancer.

4. Discussion

ZEN, known for its toxicity as an estrogen receptor activator, has been extensively studied but its multi-organ toxicity remains incompletely understood. This study aimed to investigate the mechanisms underlying ZEN-induced immunosuppression by examining the relationships between metabolites, nuclear receptors, and key targets. Metabolomic analysis revealed that ZEN exposure disrupted lipid metabolism and influenced levels of endogenous metabolites, particularly cholesterol, bile acids, and

Fig. 5. A peptide fragment of apolipoprotein E (*ApoE*) and an $\alpha 7$ nAChR antagonist ($C_{97}H_{181}N_{37}O_{19}$, COG-133) or liver X receptor (LXR-623) can alleviate the inhibitory effect of zearalenone (ZEN) on activation of T lymphocytes. (A) Flow cytometry count of T lymphocytes ($CD3^+$) in each group. (B) Flow cytometry count of Th lymphocytes ($CD3^+CD4^+$) in each group. (C) Flow cytometry count of cytotoxic T lymphocytes ($CD3^+CD8^+$) in each group ($n = 3$). The data are presented as mean \pm standard deviation (SD). Student's *t*-test was employed for all statistical analyses. Probability values with $P < 0.05$ are considered statistically significant, while probability values with $P < 0.01$ are considered extremely significant. SSC: side scatter; APC: allophycocyanin; LPS: lipopolysaccharide; FITC: fluorescein isothiocyanate; PE: phycoerythrin.

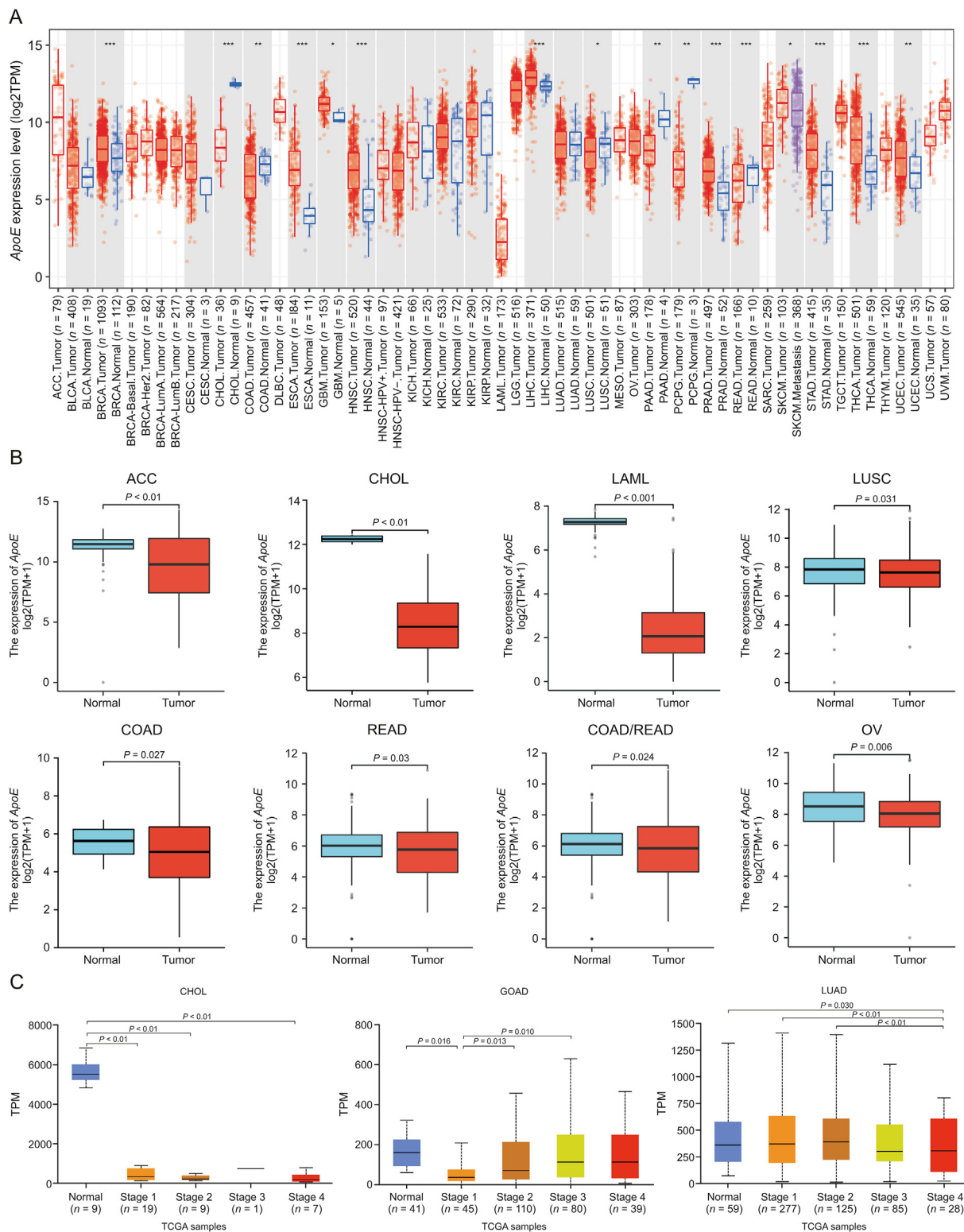


Fig. 7. Expression level of apolipoprotein E (*ApoE*) gene in different tumors and pathological stages. (A) The expression status of the *ApoE* gene in different cancers or specific cancer subtypes was analyzed through tumor immune estimation resource 2. (B) The expression status of the *ApoE* gene in *ApoE* gene low-expressed cancer was analyzed through UALCAN. (C) The expression levels of the *ApoE* gene were analyzed by the main pathological stages of cholangiocarcinoma (CHOL), colon adenocarcinoma (COAD), and lung adenocarcinoma (LUAD) based on individual cancer stages. * $P < 0.05$; ** $P < 0.01$; and *** $P < 0.001$. log₂(TPM+1) was applied for log-scale. TPM: transcripts per kilobase of exon model per million mapped reads; ACC: adrenocortical carcinoma; BLCA: bladder urothelial carcinoma; BRCA: breast invasive carcinoma; CESC: cervical squamous cell carcinoma and endocervical adenocarcinoma; DLBC: lymphoid neoplasm diffuse large B-cell lymphoma; ESCA: esophageal carcinoma; GBM: glioblastoma multiforme; HNSC: head and neck squamous cell carcinoma; HPV: human papilloma virus; KICH: kidney chromophobe; KIRC: kidney renal clear cell carcinoma; KIRP: kidney renal papillary cell carcinoma; LAML: acute myeloid leukemia; LGG: brain lower grade glioma; LIHC: liver hepatocellular carcinoma; LUSC: lung adenocarcinoma; MESO: mesothelioma; OV: ovarian serous cystadenocarcinoma; PAAD: pancreatic adenocarcinoma; PCPG: pheochromocytoma and paraganglioma; PRAD: prostate adenocarcinoma; READ: rectum adenocarcinoma; SARC: sarcoma; SKCM: skin cutaneous melanoma; STAD: stomach adenocarcinoma; TGCT: testicular germ cell tumors; THCA: thyroid carcinoma; THYM: thymoma; UCEC: uterine corpus endometrial carcinoma; UCS: uterine carcinosarcoma; UVM: uveal melanoma; FPKM: fragments per kilobase of transcript per million mapped reads; TCGA: The Cancer Genome Atlas.

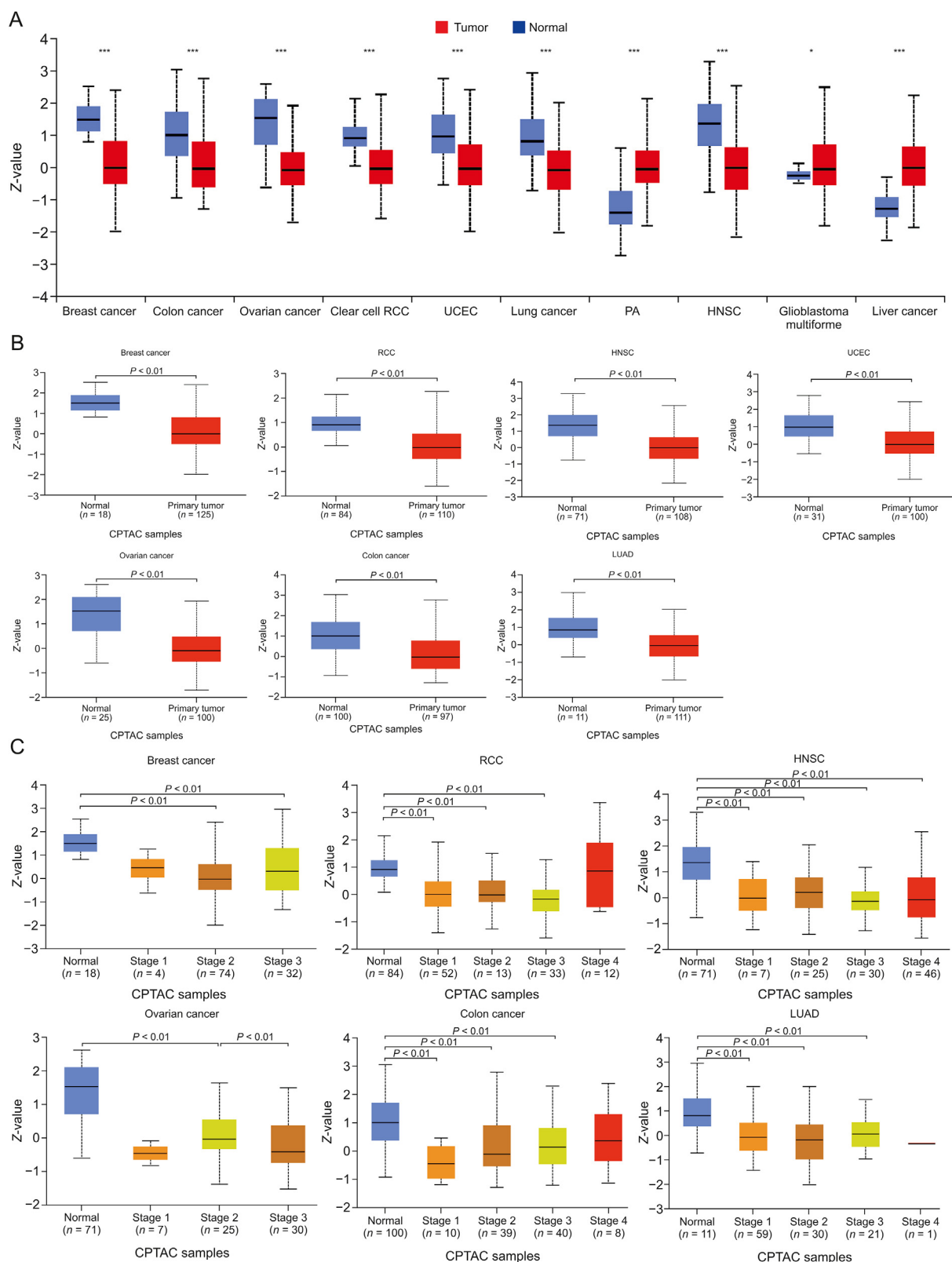


Fig. 8. Expression level of apolipoprotein E (ApoE) protein in different tumors and pathological stages. (A) The expression status of the ApoE protein in different cancers or specific cancer subtypes was analyzed through UALCAN. (B) The expression status of the ApoE protein or ApoE protein low-expressed cancer was analyzed through UALCAN. (C) The expression levels of the ApoE protein were analyzed by the main pathological stages of breast cancer, renal cell carcinoma (RCC), head and neck squamous cell carcinoma (HNSC), ovarian cancer, colon cancer, and lung adenocarcinoma (LUAD). * $P < 0.05$; ** $P < 0.01$; and *** $P < 0.001$. UCEC: uterine corpus endometrial carcinoma; PA: pilocytic astrocytoma; CPTAC: Clinical Proteomic Tumor Analysis Consortium.

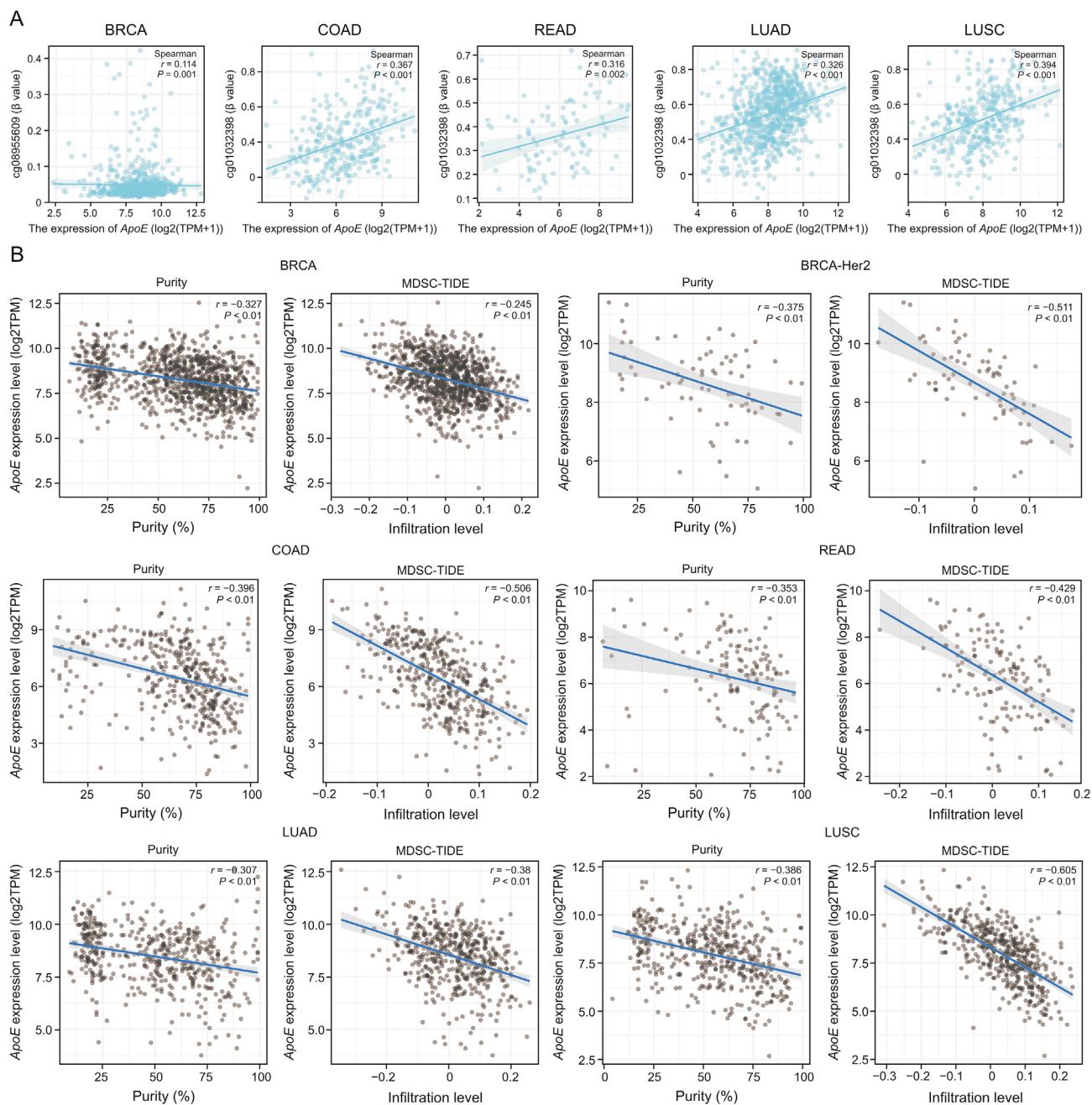


Fig. 9. The potential correlation between apolipoprotein E (*ApoE*) gene expression and DNA methylation or immune infiltration of myeloid-derived suppressor cells (MDSCs) in breast cancer, colorectal cancer, and lung cancer. (A) The potential correlation between *ApoE* gene expression and DNA methylation in breast invasive carcinoma (BRCA), colon adenocarcinoma (COAD), rectum adenocarcinoma (READ), lung adenocarcinoma (LUAD), and lung squamous cell carcinoma (LUSC). (B) The potential correlation between *ApoE* gene expression and tumor purity and immune infiltration of MDSCs in BRCA, BRCA-human epidermal growth factor receptor 2 (Her2), COAD, READ, LUAD, and LUSC. The data are presented as mean \pm standard deviation (SD). Student's *t*-test was employed for all statistical analyses. Probability values with $P < 0.05$ are considered statistically significant, while probability values with $P < 0.01$ are considered extremely significant. TPM: transcripts per kilobase of exon model per million mapped reads; MDSC-TIDE: myeloid-derived suppressor cells-tumor immune dysfunction and exclusion.

ω -3 unsaturated fatty acids. Proteomic analysis demonstrated that ZEN affected sterol and steroid synthesis and metabolism, with *ApoE* downregulation playing a crucial role in ZEN-induced intestinal immunotoxicity. Our experimental findings indicated that ZEN promotes the proliferation of MDSCs and suppresses T lymphocytes by regulating 27-HC, LXR α , and *ApoE*. Previous research has shown that unsaturated fatty acids enhance signaling protein aggregation at membranes, facilitating rapid activation of CD4 $^{+}$ T cells [62]. Conversely, ZEN-induced downregulation of ω -3 unsaturated fatty acids exacerbates T lymphocyte inactivation. Through examination of the metabolite/nuclear receptor/key

target axis, we elucidated the mechanisms of ZEN-induced immunosuppression in the intestine and identified new avenues for toxicological studies of ZEN.

Although ZEN was classified as a class 3 carcinogen in 2017, recent toxicology studies have underscored its carcinogenic potential. Two case-control studies conducted in Africa investigated the association between ZEN and its metabolites with breast cancer risk, yielding conflicting results [60]. Pajewska et al. [63] detected ZEN and its metabolites in 47 out of 61 endometrial cancer patient tissue samples, indirectly suggesting a link between endometrial cancer and ZEN exposure. In addition to estrogen-sensitive cancers, a study

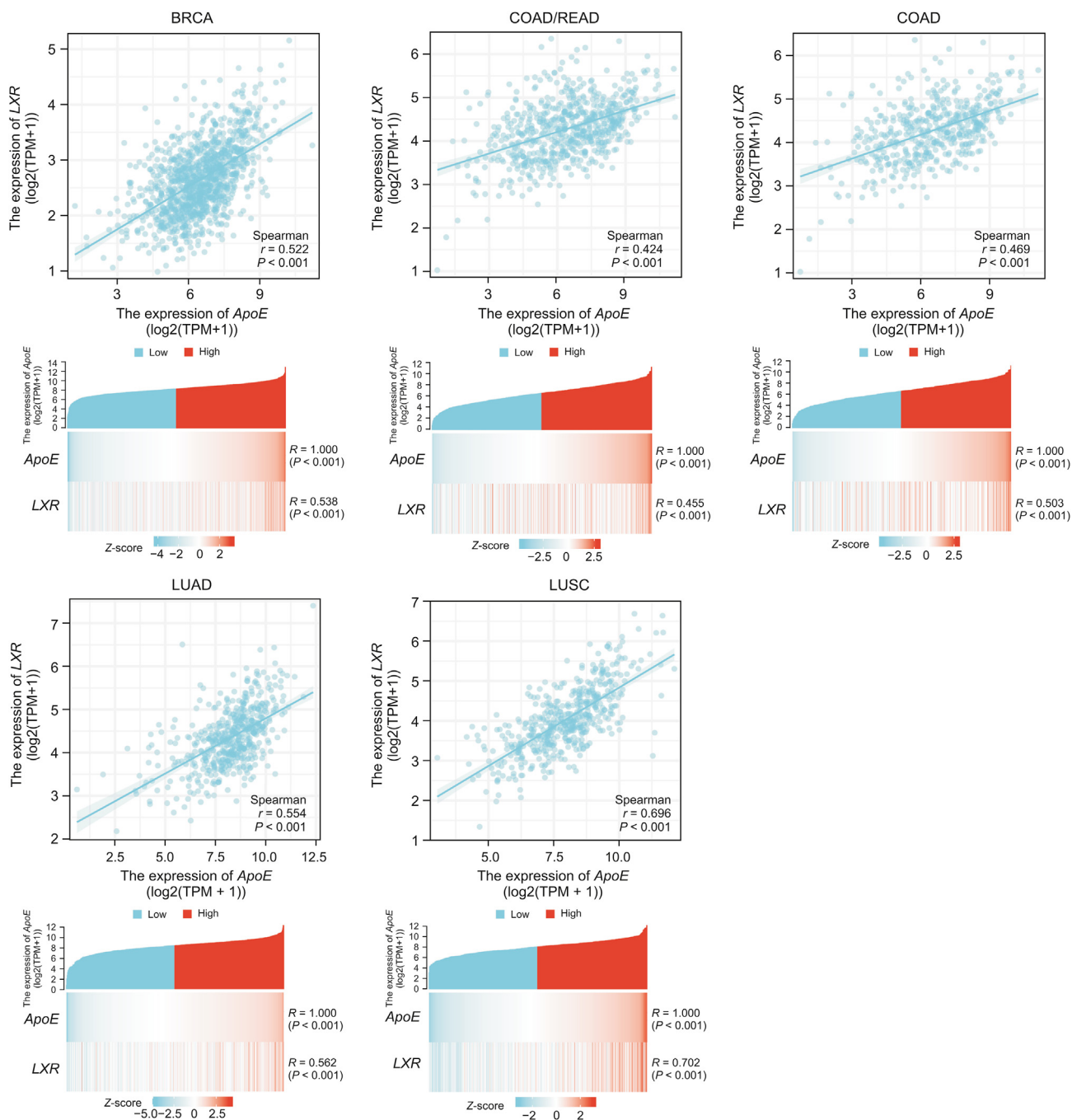


Fig. 10. The potential correlation between apolipoprotein E (*ApoE*) and liver X receptor (*LXR*) gene expression in breast invasive carcinoma (BRCA), colon adenocarcinoma (COAD)/rectum adenocarcinoma (READ), COAD, lung adenocarcinoma (LUAD), and lung squamous cell carcinoma (LUSC). The data are presented as mean \pm standard deviation (SD). Student's *t*-test was employed for all statistical analyses. Probability values $P < 0.001$ are considered extremely significant. TPM: transcripts per kilobase of exon model per million mapped reads.

from Poland was the first to establish a connection between dietary ZEN exposure and colorectal cancer development [64]. Moreover, Lo et al. [65] demonstrated that ZEN promoted the growth of colon cancer cells. Additionally, MDSCs play a significant role in the immune microenvironment during chronic inflammation or tumor development, contributing to inflammation and tumor progression through immunosuppression [66]. Our study revealed that ZEN enhances MDSCs proliferation in the intestine by inhibiting ApoE, opening new avenues for a comprehensive exploration of ZEN's carcinogenic properties. Through our pan-cancer analysis of ApoE, we found that ZEN exposure may increase or accelerate the risk and

pathological progression of breast, lung, and colorectal cancers. Single-cell analysis further highlighted the pivotal role of ApoE in colorectal cancer, thereby supporting the hypothesis that ZEN exposure detrimentally affects colorectal cancer.

As a complex neurodegenerative disorder, AD involves dysregulation of numerous cellular and molecular processes, and its primary cause remains unclear. Genome-wide association studies have identified the *ApoE* $\epsilon 4$ allele (*ApoE4*) as the most significant genetic risk factor for AD [67]. Additionally, extensive epidemiological data have linked ω -3 unsaturated fatty acid levels to AD risk [68]. The multidomain Alzheimer preventive trial demonstrated

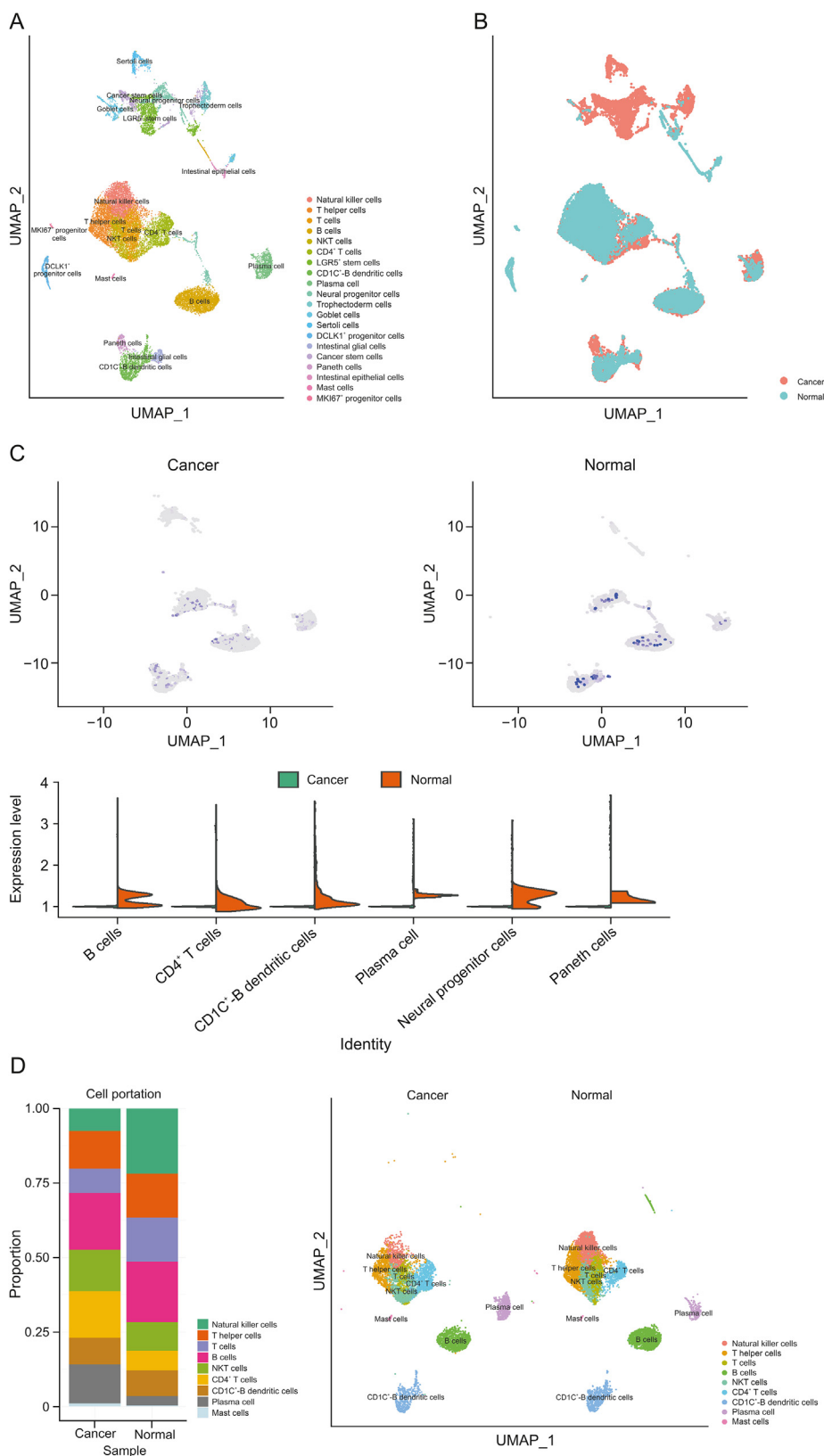


Fig. 11. Expression of apolipoprotein E (*ApoE*) in different cell lineages of colorectal cancer. (A) Cells are grouped by uniform manifold approximation and projection (UMAP) method and manually annotated, and different numbers or colors represent different cell groups. (B) Distribution of cells detected in cancer or normal tissue. (C) Expression of *ApoE* in B cells, CD4⁺ T cells, CD1C⁺-B dendritic cells, plasma cells, neural progenitor cells, and paneth cells in cancer and normal tissues. (D) The proportion of different immune cells in cancer or normal tissue.

that intake of ω -3 unsaturated fatty acids improved cognitive function in individuals with positive amyloid levels [69]. Another study suggested that docosahexaenoic acid (DHA) supplementation could benefit *ApoE4* carriers before the onset of AD dementia [70]. In the past decade, substantial evidence has emerged linking mycotoxins to neurotoxicity and neurodegenerative diseases [71]. A recent study indicated a connection between ZEN-induced mitochondrial fragmentation, apoptosis, and potential harm to individuals with Parkinson's disease [72]. In our study, we conducted metabolomic analysis of rat serum and observed that ZEN exposure significantly reduced eicosapentaenoic acid (EPA) and DHA levels (Fig. 2H and Table S1), impairing ω -3 unsaturated fatty acid synthesis and metabolism. These findings suggest that dietary ZEN exposure may increase the risk of AD. Although our study demonstrated histopathological changes and significant effects on *ApoE* expression in the liver and brain of rats exposed to ZEN (Figs. S9A–C), it remains unclear whether ZEN causes *ApoE4* gene mutation. Further comprehensive investigations into the effects of ZEN on the brain are necessary to determine the relationship between dietary ZEN exposure and AD, and to explore new strategies for AD prevention and treatment.

With advances in exogenous pollutant analysis technology and improvements in food and drug quality supervision, acute food poisoning caused by mycotoxins has gradually declined, although sporadic cases still occur in recent years [73]. Moreover, mycotoxins in animal feed severely impact animal growth and health [74]. Research has shown that the incidence of ZEN in animal feed in China between 2018 and 2020 ranged from 96.9% to 100%, with contamination levels of 226.0–1599.0 $\mu\text{g}/\text{kg}$ [75]. A 2021 report demonstrated a 47% incidence of ZEN in pig feed in the United States [76]. Residues from ZEN ingestion by pigs, poultry, and ruminants can enter the human body through food consumption, posing a risk to public health. However, there is currently no clinical drug available to prevent or treat acute and chronic ZEN poisoning. Our results indicated that LXR agonists or *ApoE* could mitigate ZEN-induced immunotoxicity. We believe that dietary supplementation of 27-HC and the administration of LXR agonists or *ApoE* may prevent or treat ZEN immunotoxicity in high-risk populations and susceptible animals. These findings present a new avenue for research aimed at developing clinical diagnosis and treatment methods for acute and chronic ZEN poisoning.

However, the dose of ZEN (5 mg/kg/day, 14 days) used in the rat model we established exceeded the human exposure dose. Our current experimental results reflect the impact of ZEN exposure on rats in a basic laboratory research setting and can only offer ideas and directions for future research on the potential relationship between ZEN exposure and human diseases. To establish a more specific relationship between ZEN exposure and diseases, it is necessary to develop a long-term low-dose exposure model for ZEN and further explore its effects. Our future research will focus on utilizing a ZEN long-term low-dose exposure model to address the findings of this experiment.

5. Conclusion

ZEN has garnered attention among researchers as an estrogen-like mycotoxin that contaminates food and feed extensively, yet its mechanism of immunotoxicity in the intestine remains unclear. Recently, we have become particularly interested in the severe lipid disorders induced by ZEN as an environmental endocrine disruptor in the gut. Consequently, we conducted a study examining the effect of ZEN exposure on the serum metabolomics and intestinal proteomics of rats. Through combined pathological experiments, we discovered that ZEN promotes the proliferation of MDSCs by regulating the 27-HC/LXRs/

ApoE axis, thereby inhibiting the activation of T lymphocytes in the rat intestine. Furthermore, bioinformatics analysis indicated that ZEN exposure may increase or accelerate the risk of breast cancer, lung cancer, and colorectal cancer. This study elucidates the mechanism of ZEN-induced intestinal immunosuppression and highlights a potential association between ZEN exposure and cancer, providing a theoretical basis for the prevention of ZEN poisoning and the improvement of ZEN limit standards in food and feed.

CRedit author statement

Haonan Ruan: Writing - Original draft preparation, Data curation, Investigation, Software, Validation; **Jing Zhang:** Writing - Reviewing and Editing, Data curation, Software; **Yunyun Wang:** Data curation, Visualization, Formal analysis; **Ying Huang:** Data curation, Validation; **Jiashuo Wu:** Methodology, Software; **Chunjiao He:** Software; **Tongwei Ke:** Data curation; **Jiaoyang Luo:** Resources, Supervision, Conceptualization, Writing - Reviewing and Editing; **Meihua Yang:** Project administration, Supervision, Funding acquisition, Writing - Reviewing and Editing.

Declaration of competing interest

The authors declare that there are no conflicts of interest.

Acknowledgments

This study was supported by the Fundamental Research Funds for the Central Universities, China (Grant No.: 3332022147), the CAMS Innovation Fund for Medical Sciences, China (Grant Nos.: 2021-I2M-1-071 and 2021-I2M-1-031), and the National Natural Science Foundation of China (Grant No.: 81872999).

Appendix A. Supplementary data

Supplementary data to this article can be found online at <https://doi.org/10.1016/j.jpha.2023.08.002>.

References

- [1] A. Rai, M. Das, A. Tripathi, Occurrence and toxicity of a fusarium mycotoxin, zearalenone, Crit. Rev. Food Sci. Nutr. 60 (2020) 2710–2729.
- [2] J. Bai, Y. Zhou, X. Luo, et al., Roles of stress response-related signaling and its contribution to the toxicity of zearalenone in mammals, Compr. Rev. Food Sci. Food Saf. 21 (2022) 3326–3345.
- [3] K. Ropejko, M. Twarużek, Zearalenone and its metabolites – General overview, occurrence, and toxicity, Toxins 13 (2021), 35.
- [4] C. Arnold, Tracking zearalenone: Placental transfer of a fungal toxin, Environ. Health Perspect. 128 (2020), 74001.
- [5] H. Ruan, Q. Lu, J. Wu, et al., Hepatotoxicity of food-borne mycotoxins: Molecular mechanism, anti-hepatotoxic medicines and target prediction, Crit. Rev. Food Sci. Nutr. 62 (2022) 2281–2308.
- [6] E. Commission, Presence of Deoxynivalenol, Zearalenone, Ochratoxin A, T-2 and HT-2 and Fumonisin in Products Intended for Animal Feeding, August 17, 2006, Brussels, Belgium, 2006.
- [7] S. Zhang, S. Zhou, Y.Y. Gong, et al., Human dietary and internal exposure to zearalenone based on a 24-hour duplicate diet and following morning urine study, Environ. Int. 142 (2020), 105852.
- [8] K. De Ruyck, I. Huybrechts, S. Yang, et al., Mycotoxin exposure assessments in a multi-center European validation study by 24-hour dietary recall and biological fluid sampling, Environ. Int. 137 (2020), 105539.
- [9] S. Marin, A.J. Ramos, G. Cano-Sancho, et al., Mycotoxins: Occurrence, toxicology, and exposure assessment, Food Chem. Toxicol. 60 (2013) 218–237.
- [10] L. Toporova, P. Balaguer, Nuclear receptors are the major targets of endocrine disrupting chemicals, Mol. Cell. Endocrinol. 502 (2020), 110665.
- [11] F. Lai, X. Liu, N. Li, et al., Phosphatidylcholine could protect the defect of zearalenone exposure on follicular development and oocyte maturation, Aging 10 (2018) 3486–3506.
- [12] T. Wang, Y. Ye, J. Ji, et al., Diet composition affects long-term zearalenone exposure on the gut-blood-liver axis metabolic dysfunction in mice, Ecotoxicol. Environ. Saf. 236 (2022), 113466.

- [13] H. Wang, Y. Xiao, C. Xu, et al., Integrated metabolomics and transcriptomics analyses reveal metabolic mechanisms in porcine intestinal epithelial cells under zearalenone stress, *J. Agric. Food Chem.* 70 (2022) 6561–6572.
- [14] Y. Sun, K. Huang, M. Long, et al., An update on immunotoxicity and mechanisms of action of six environmental mycotoxins, *Food Chem. Toxicol.* 163 (2022), 112895.
- [15] W. Fan, Y. Lv, S. Ren, et al., Zearalenone (ZEA)-induced intestinal inflammation is mediated by the NLRP3 inflammasome, *Chemosphere* 190 (2018) 272–279.
- [16] A.M. Mowat, W.W. Agace, Regional specialization within the intestinal immune system, *Nat. Rev. Immunol.* 14 (2014) 667–685.
- [17] G. Cai, S. Xia, F. Zhong, et al., Zearalenone and deoxynivalenol reduced Th1-mediated cellular immune response after *Listeria monocytogenes* infection by inhibiting CD4⁺ T cell activation and differentiation, *Environ. Pollut.* 284 (2021), 117514.
- [18] L. Soler, A. Stella, J. Seva, et al., Proteome changes induced by a short, non-cytotoxic exposure to the mycoestrogen zearalenone in the pig intestine, *J. Proteom.* 224 (2020), 103842.
- [19] H. Zhang, Y. Wang, X. Zhou, et al., Zearalenone induces immuno-compromised status via TOR/NF κ B pathway and aggravates the spread of *Aeromonas hydrophila* to grass carp gut (*Ctenopharyngodon idella*), *Ecotoxicol. Environ. Saf.* 225 (2021), 112786.
- [20] F. Wu, J.D. Groopman, J.J. Pestka, Public health impacts of foodborne mycotoxins, *Annu. Rev. Food Sci. Technol.* 5 (2014) 351–372.
- [21] J.M. Llovet, J. Zucman-Rossi, E. Pikarsky, et al., Hepatocellular carcinoma, *Nat. Rev. Dis. Primers* 2 (2016), 16018.
- [22] V. Ostry, F. Malir, J. Toman, et al., Mycotoxins as human carcinogens—the IARC Monographs classification, *Mycotoxin Res.* 33 (2017) 65–73.
- [23] D.E. Bredesen, Inhalational Alzheimer's disease: An unrecognized—and treatable—epidemic, *Aging* 8 (2016) 304–313.
- [24] D. Payros, S. Ménard, J. Laffitte, et al., The food contaminant, deoxynivalenol, modulates the Thelper/Treg balance and increases inflammatory bowel diseases, *Arch. Toxicol.* 94 (2020) 3173–3184.
- [25] J.X. Hu, C.E. Thomas, S. Brunak, Network biology concepts in complex disease comorbidities, *Nat. Rev. Genet.* 17 (2016) 615–629.
- [26] G. Miao, D. Zhuo, X. Han, et al., From degenerative disease to malignant tumors: Insight to the function of ApoE, *Biomed. Pharmacother.* 158 (2023), 114127.
- [27] B. Hui, C. Lu, H. Li, et al., Inhibition of APOE potentiates immune checkpoint therapy for cancer, *Int. J. Biol. Sci.* 18 (2022) 5230–5240.
- [28] A. Serrano-Pozo, S. Das, B.T. Hyman, APOE and Alzheimer's disease: Advances in genetics, pathophysiology, and therapeutic approaches, *Lancet Neurol.* 20 (2021) 68–80.
- [29] C. Liu, Z. Li, Z. Song, et al., Choline and butyrate beneficially modulate the gut microbiome without affecting atherosclerosis in *APOE*3-Leiden.CETP* mice, *Atherosclerosis* 362 (2022) 47–55.
- [30] A.M. Bea, F. Civeira, V. Marco-Benedí, et al., Contribution of *APOE* genetic variants to dyslipidemia, *Atherosclerosis* 355 (2022), 175.
- [31] K. Mao, A.P. Baptista, S. Tamoutounour, et al., Innate and adaptive lymphocytes sequentially shape the gut microbiota and lipid metabolism, *Nature* 554 (2018) 255–259.
- [32] W. Zhang, S. Zhang, J. Wang, et al., Changes in intestinal barrier functions and gut microbiota in rats exposed to zearalenone, *Ecotoxicol. Environ. Saf.* 204 (2020), 111072.
- [33] Y. Li, Q. Kong, J. Yue, et al., Genome-edited skin epidermal stem cells protect mice from cocaine-seeking behaviour and cocaine overdose, *Nat. Biomed. Eng.* 3 (2019) 105–113.
- [34] W. Zhou, C. Chen, Y. Shi, et al., Targeting glioma stem cell-derived pericytes disrupts the blood-tumor barrier and improves chemotherapeutic efficacy, *Cell Stem Cell* 21 (2017) 591–603.e4.
- [35] O. Maller, A.P. Drain, A.S. Barrett, et al., Tumour-associated macrophages drive stromal cell-dependent collagen crosslinking and stiffening to promote breast cancer aggression, *Nat. Mater.* 20 (2021) 548–559.
- [36] S.C. Baksh, P.K. Todorova, S. Gur-Cohen, et al., Extracellular serine controls epidermal stem cell fate and tumour initiation, *Nat. Cell Biol.* 22 (2020) 779–790.
- [37] Y. Jing, L. Luo, Y. Chen, et al., SARS-CoV-2 infection causes immunodeficiency in recovered patients by downregulating CD19 expression in B cells via enhancing B-cell metabolism, *Signal Transduct. Target. Ther.* 6 (2021), 345.
- [38] M. Wang, Z. Zhang, J. Liu, et al., Gefitinib and fostamatinib target EGFR and SYK to attenuate silicosis: A multi-omics study with drug exploration, *Signal Transduct. Target. Ther.* 7 (2022), 157.
- [39] A. Florido, E.R. Velasco, C.M. Soto-Faguás, et al., Sex differences in fear memory consolidation via Tac2 signaling in mice, *Nat. Commun.* 12 (2021), 2496.
- [40] Y. Liu, X. Liang, W. Dong, et al., Tumor-repopulating cells induce PD-1 expression in CD8⁺ T cells by transferring kynurenine and AhR activation, *Cancer Cell* 33 (2018) 480–494.e7.
- [41] C. Sun, P. Shou, H. Du, et al., THEMIS-SHP1 recruitment by 4-1BB tunes LCK-mediated priming of chimeric antigen receptor-redirected T cells, *Cancer Cell* 37 (2020) 216–225.e6.
- [42] T. Li, J. Fu, Z. Zeng, et al., TIMER2.0 for analysis of tumor-infiltrating immune cells, *Nucleic Acids Res.* 48 (2020) W509–W514.
- [43] D.S. Chandrashekar, B. Bashel, S.A.H. Balasubramanya, et al., UALCAN: A portal for facilitating tumor subgroup gene expression and survival analyses, *Neoplasia* 19 (2017) 649–658.
- [44] M. Ju, J. Bi, Q. Wei, et al., Pan-cancer analysis of NLRP3 inflammasome with potential implications in prognosis and immunotherapy in human cancer, *Brief. Bioinform.* 22 (2021), bbaa345.
- [45] E. Cerami, J. Gao, U. Dogrusoz, et al., The cBio cancer genomics portal: An open platform for exploring multidimensional cancer genomics data, *Cancer Discov.* 2 (2012) 401–404.
- [46] W.M. Song, P. Agrawal, R. Von Itter, et al., Network models of primary melanoma microenvironments identify key melanoma regulators underlying prognosis, *Nat. Commun.* 12 (2021), 1214.
- [47] D. Biswas, N.J. Birkbak, R. Rosenthal, et al., A clonal expression biomarker associates with lung cancer mortality, *Nat. Med.* 25 (2019) 1540–1548.
- [48] J.R. Evans, S.G. Zhao, S.L. Chang, et al., Patient-level DNA damage and repair pathway profiles and prognosis after prostatectomy for high-risk prostate cancer, *JAMA Oncol.* 2 (2016) 471–480.
- [49] J. Hu, Z. Chen, L. Bao, et al., Single-cell transcriptome analysis reveals intratumoral heterogeneity in cRCC, which results in different clinical outcomes, *Mol. Ther.* 28 (2020) 1658–1672.
- [50] X. Liu, S. Jin, S. Hu, et al., Single-cell transcriptomics links malignant T cells to the tumor immune landscape in cutaneous T cell lymphoma, *Nat. Commun.* 13 (2022), 1158.
- [51] X. Zhang, Y. Lan, J. Xu, et al., CellMarker: A manually curated resource of cell markers in human and mouse, *Nucleic Acids Res.* 47 (2019) D721–D728.
- [52] G. Cai, K. Sun, T. Wang, et al., Mechanism and effects of zearalenone on mouse T lymphocytes activation *in vitro*, *Ecotoxicol. Environ. Saf.* 162 (2018) 208–217.
- [53] M.N. Bradley, C. Hong, M. Chen, et al., Ligand activation of LXR β reverses atherosclerosis and cellular cholesterol overload in mice lacking LXR α and apoE, *J. Clin. Invest.* 117 (2007) 2337–2346.
- [54] M.F. Tavazoie, I. Pollack, R. Tanqueco, et al., LXR/ApoE activation restricts innate immune suppression in cancer, *Cell* 172 (2018) 825–840.e18.
- [55] H. Wu, Y. Zhen, Z. Ma, et al., Arginase-1-dependent promotion of TH17 differentiation and disease progression by MDSCs in systemic lupus erythematosus, *Sci. Transl. Med.* 8 (2016), 331ra40.
- [56] E.R. Nelson, S.E. Wardell, J.S. Jasper, et al., 27-Hydroxycholesterol links hypercholesterolemia and breast cancer pathophysiology, *Science* 342 (2013) 1094–1098.
- [57] D. Killock, Immunotherapy: Targeting MDSCs with LXR agonists, *Nat. Rev. Clin. Oncol.* 15 (2018) 200–201.
- [58] V. Kumar, Q. Wang, B. Sethi, et al., Polymeric nanomedicine for overcoming resistance mechanisms in hedgehog and Myc-amplified medulloblastoma, *Biomaterials* 278 (2021), 121138.
- [59] G.R. Villa, J.J. Hulce, C. Zanca, et al., An LXR-cholesterol axis creates a metabolic co-dependency for brain cancers, *Cancer Cell* 30 (2016) 683–693.
- [60] L. Claeys, C. Romano, K. De Ruycck, et al., Mycotoxin exposure and human cancer risk: A systematic review of epidemiological studies, *Compr. Rev. Food Sci. Food Saf.* 19 (2020) 1449–1464.
- [61] E.K.K. Lo, X. Wang, P.K. Lee, et al., Mechanistic insights into zearalenone-accelerated colorectal cancer in mice using integrative multi-omics approaches, *Comput. Struct. Biotechnol. J.* 21 (2023) 1785–1796.
- [62] T.Y. Hou, D.N. McMurray, R.S. Chapkin, Omega-3 fatty acids, lipid rafts, and T cell signaling, *Eur. J. Pharmacol.* 785 (2016) 2–9.
- [63] M. Pajewska, M. Łojko, K. Cendrowski, et al., The determination of zearalenone and its major metabolites in endometrial cancer tissues, *Anal. Bioanal. Chem.* 410 (2018) 1571–1582.
- [64] K.E. Przybyłowicz, T. Artukowicz, A. Danielewicz, et al., Association between mycotoxin exposure and dietary habits in colorectal cancer development among a Polish population: A study protocol, *Int. J. Environ. Res. Public Health* 17 (2020), 698.
- [65] E.K.K. Lo, J.C.Y. Lee, P.C. Turner, et al., Low dose of zearalenone elevated colon cancer cell growth through G protein-coupled estrogenic receptor, *Sci. Rep.* 11 (2021), 7403.
- [66] F. Veglia, M. Perego, D. Gabrilovich, Myeloid-derived suppressor cells coming of age, *Nat. Immunol.* 19 (2018) 108–119.
- [67] C. Wang, R. Najm, Q. Xu, et al., Gain of toxic apolipoprotein E4 effects in human iPSC-derived neurons is ameliorated by a small-molecule structure corrector, *Nat. Med.* 24 (2018) 647–657.
- [68] D.R. Gustafson, K. Bäckman, N. Scarmeas, et al., Dietary fatty acids and risk of Alzheimer's disease and related dementias: Observations from the Washington Heights-Hamilton Heights-Inwood Columbia Aging Project (WHICAP), *Alzheimers. Dement.* 16 (2020) 1638–1649.
- [69] J. Delrieu, P. Payoux, I. Carrié, et al., Multidomain intervention and/or omega-3 in nondemented elderly subjects according to amyloid status, *Alzheimers Dement.* 15 (2019) 1392–1401.
- [70] H.N. Yassine, M.N. Braskie, W.J. Mack, et al., Association of docosahexaenoic acid supplementation with Alzheimer disease stage in apolipoprotein E ϵ 4 carriers: A review, *JAMA Neurol.* 74 (2017) 339–347.
- [71] X. Pei, W. Zhang, H. Jiang, et al., Food-origin mycotoxin-induced neurotoxicity: Intend to break the rules of neuroglia cells, *Oxid. Med. Cell. Longev.* 2021 (2021), 9967334.

- [72] C.C. Wei, N.C. Yang, C. Huang, Zearalenone induces dopaminergic neurodegeneration via DRP-1-involved mitochondrial fragmentation and apoptosis in a *Caenorhabditis elegans* Parkinson's disease model, *J. Agric. Food Chem.* 69 (2021) 12030–12038.
- [73] F. Ruan, J.G. Chen, L. Chen, et al., Food poisoning caused by deoxynivalenol at a school in Zhuhai, Guangdong, China, in 2019, *Foodborne Pathog. Dis.* 17 (2020) 429–433.
- [74] C. Yang, G. Song, W. Lim, Effects of mycotoxin-contaminated feed on farm animals, *J. Hazard. Mater.* 389 (2020), 122087.
- [75] L. Zhao, L. Zhang, Z. Xu, et al., Occurrence of aflatoxin B₁, deoxynivalenol and zearalenone in feeds in China during 2018–2020, *J. Anim. Sci. Biotechnol.* 12 (2021), 74.
- [76] E.D. Pack, S. Weiland, R. Musser, et al., Survey of zearalenone and type-B trichothecene mycotoxins in swine feed in the USA, *Mycotoxin Res.* 37 (2021) 297–313.